2-P(mix)

USTS HC $3.75

NASA TECHNICAL MEMORANDUM

NASA TM X-62,117

[redacted]

NASA TM X-62,117

PRESSURE SIGNATURES FOR THE APOLLO COMMAND MODULE AND THE SATURN V LAUNCH VEHICLE WITH A DISCUSSION OF STRONG SHOCK EXTRAPOLATION PROCEDURES

Raymond M. Hicks, Joel P. Mendoza, and Charles L. Thomas

Ames Research Center
Moffett Field, Ca., 94035

April 1972

PRESSURE SIGNATURES FOR THE APOLLO COMMAND MODULE AND THE SATURN V LAUNCH VEHICLE WITH A DISCUSSION OF STRONG SHOCK EXTRAPOLATION PROCEDURES

By Raymond M. Hicks, Joel P. Mendoza and Charles L. Thomas
Ames Research Center

ABSTRACT

Wind tunnel pressure signatures measured at Mach 10.1 for a model of the Apollo Command Module and at Mach numbers from 3.01 to 7.91 for two models of the Saturn launch configuration are presented. The signatures for the command module were obtained at roll angles ranging from 0° to 180°. A brief discussion of the extrapolation of strong pressure signatures is included in the report.

SYMBOLS

a	sound speed, m/sec
d	diameter of Apollo model, m
h	altitude, m
K_r	reflection factor (see figure 19)
l	length of Saturn model, m (see figure 2)
M	Mach number
p	reference pressure, N/m^2
u	fluid particle speed, m/sec
U_s	shock speed, m/sec
α	angle of attack, deg.
γ	ratio of specific heats
Δp	sonic boom overpressure, N/m^2
Δx	axial distance from bow shock, m
θ	shock angle, deg
ϕ	roll angle, deg
ρ	density, Kg/m^3

Subscripts

1	value ahead of incident shock
2	value behind incident shock
3	value behind reflected shock
r	reference value
s	shock value
∞	free stream value

PRESSURE SIGNATURES FOR THE APOLLO COMMAND MODULE AND THE SATURN V LAUNCH VEHICLE WITH A DISCUSSION OF STRONG SHOCK EXTRAPOLATION PROCEDURES

By Raymond M. Hicks, Joel P. Mendoza and Charles L. Thomas
Ames Research Center

SUMMARY

Wind tunnel tests were conducted to obtain pressure signatures for a .016-scale model of the Apollo Command Module, a .00337 and a .00168-scale model of the Saturn V launch vehicle. The pressure signatures for the command module were measured at Mach 10.1 whereas the signatures for the Saturn were obtained over a Mach number range from 3.01 to 7.91. Data were obtained at roll angles from 0° to 180° in 30° increments for the command module. The Saturn was tested with three different sizes of simulated exhaust plumes and without plume. Because of the large values of pressure $\left(\frac{\Delta p}{p} > .5\right)$ recorded at the hypersonic Mach numbers a method for extrapolating strong pressure signatures is included herein.

INTRODUCTION

An investigation is underway to evaluate the Ames sonic boom extrapolation program (ref. 1) for accelerated flight at hypersonic Mach numbers. The initial phase of this evaluation consisted of a correlation of extrapolated wind tunnel pressure signatures with flight data recorded during reentry of the Apollo 15 Command Module (ref. 2). However, the highest Mach number for which flight data were obtained was 4.57. Hence, the only high Mach number information, in addition to that presented in refs. 3 and 4 for the XB-70 and X-15 airplanes, provided by the Apollo experiment was a check on the ability of the Ames extrapolation program to predict sonic boom levels for accelerated flight. The results of this initial correlation were encouraging and hence an additional wind tunnel-flight correlation is planned for the Apollo 16 mission.

During the Apollo 16 mission pressure signatures will be recorded along the ground track during both the launch and reentry phases. These flight pressure signatures will be compared with predictions based on extrapolations of the wind tunnel data presented in this report. An effort will be made to locate sonic boom recording equipment at a position along the reentry ground track so as to record a pressure signature generated by the command module at a Mach number greater than 8. This should provide

the additional information required to establish the validity of the Ames sonic boom extrapolation program for hypersonic Mach numbers.

An additional aspect of the investigation is to provide information as to the appropriate size solid body required to simulate an actual exhaust plume for rocket powered launch vehicles. This information will be provided by comparing extrapolations of the wind tunnel pressure signatures for the Saturn V model with different plume sizes presented herein with signatures measured along the ground track of the Saturn V during the launch phase of the mission.

Some of the pressure signatures presented here and in reference 2 for hypersonic Mach numbers exhibit large values of overpressure $\left(\frac{\Delta p}{p} > .5 \right)$. The extrapolation of such signatures requires a somewhat different approach than that used for weak shock waves. A technique for strong-shock extrapolation is presented in the appendix of this report.

MODEL AND TEST PROCEDURE

A .016-scale model of the Apollo Command Module was tested in the .533 m. hypersonic wind tunnel of the Jet Propulsion Laboratory. A sketch of the model and sting at the zero-roll-angle position is shown in figure 1. The roll axis is colinear with the velocity vector for both the model and the spacecraft. The roll angle is specified as the angle between the pitch plane of the model and the vertical plane containing the centerlines of the model sting and the overpressure probe. Pressure signatures were obtained at Mach 10.1 for roll angles from 0° to 180° in increments of 30°. The angle of attack and total pressure used for tests of the Apollo Command Module were 25° and 1500 cm-Hg respectively.

Two different size models (.00337 scale and .00168 scale) of the Saturn V launch vehicle complete with Apollo Command Module, escape tower and 3 different size simulated exhaust plumes were tested in the .508 m. supersonic and the .533 m. hypersonic wind tunnels of the Jet Propulsion Laboratory. A sketch and photographs of the models are shown in figures 2 and 3, respectively. The simulated exhaust plumes were sized according to the data presented in figure 4.[1] The diameter of the largest plume corresponds to the boundary between the outer inviscid flow and the inner viscous mixing region. This is called the mixing-boundary plume. The diameters of the two smaller plumes were calculated from inviscid considerations. These are called the inviscid-boundary and 2/3 inviscid-boundary

[1]Exhaust plume dimensions were furnished by Mr. Jess Jones of the George C. Marshall Spaceflight Center.

plumes. All simulated plumes were solid aluminum cones and were attached to the sting immediately behind the models. The .00337-scale model was tested with the 2/3-inviscid-boundary plumes, the full inviscid-boundary plumes and without plume. The .00168-scale model was tested with the mixing-boundary plumes only. Both models with plumes were tested at Mach numbers of 3.01, 3.98, 4.76 and 5.56, whereas the .00337-scale model without plume was tested at the additional Mach number of 7.91. A photograph of the .00337-scale model with simulated plume installed in the .508 m. supersonic wind tunnel of the Jet Propulsion Laboratory (JPL) is shown in figure 5. The plume length had to be terminated at 1/2 model length because of blockage limitations of the wind tunnels. It was necessary to manufacture the smaller .00168-scale model to test the mixing-boundary plumes because the large model with mixing boundary plume exceeded the maximum allowable size for blockage of the JPL wind tunnels at all Mach numbers.

The total pressure for each Mach number investigated during the Saturn phase of the test is given in the table below:

M	P_t (cm-Hg)
3.01	75
3.98	100
4.76	250
5.56	600
7.91	1000

PRESENTATION OF DATA

Schlieren photographs of the Apollo Command Module taken during testing at Mach 10.1 are shown in figure 6. A photograph is shown for each roll angle from 0° to 180° to depict the asymmetry of the shock front. The overpressure probe does not appear in the photographs because it was located downstream, out of view of the window. However, its distance below the model can be ascertained since the probe centerline was located 2.85 model diameters below the centerline of the sting.

Wind tunnel pressure signatures for the Apollo Command Module recorded during testing at Mach 10.1 are shown in figure 7. Signatures were obtained at roll angles ranging from 0° to 180° in 30° increments at an

angle of attack of 25^{o} and an altitude-to-model diameter ratio of 2.85. Only the positive portion of the signature was obtainable because of the very long signature length and the limited travel of the linear actuator on which the model was mounted. However, only the positive portion of the signature is required for calculation of the maximum ground overpressures. Note the secondary shock behind the bow shock at roll angles of 0^{o}, 30^{o}, 60^{o}, 90^{o} and 120^{o} (figures 7(a) through 7(e)). This shock was previously thought to be due to sting interference as discussed in reference 2. However, tests conducted in the Ames 61 m. pressurized ballistic range show that this intermediate shock is due to a recompression behind the shoulder of the model (see figure 8). This shock could not be detected in the schlieren photographs shown in reference 2 or in the schlieren photographs of figure 6 because of the low density in the wind tunnel. The recompression shock is clearly visible in figure 8 because the density in the ballistic range is considerably greater than that in the wind tunnel. While no schlieren or shadowgraph pictures are available to show the position of the recompression shock at hypersonic Mach numbers it is apparent by comparing results in figures 7(a) and 7(b) with those in figure 9 that the recompression shock moves in the direction of the bow shock with increasing Mach number (Figure 9 is reproduced from reference 2). Hence, when extrapolating hypersonic pressure signatures it will be necessary to include the entire positive portion of the signatures of figure 7 rather than adjust the data as suggested in reference 2.

Overpressures of the magnitude found in the data of figure 7 should not be extrapolated by the method of reference 1 because of the weak wave assumptions on which the extrapolation method is based. The proper technique would be to employ a procedure applicable to strong shock waves to extrapolate the signatures of figure 7 to a distance (usually 4 or 5 model diameters) from the axis at which the overpressures reduce to levels for which the weak shock procedures are applicable. It is then possible to continue the extrapolation by use of the method of reference 1 to the far field (ground level). A procedure for the extrapolation of strong pressure signatures is given in the Appendix.

Schlieren photographs of the Saturn V models with the three different plume sizes and without plume are shown in figures 10 through 13.

The wind tunnel pressure signatures for the .00337-scale Saturn model without simulated plume at Mach numbers of 3.01, 3.98, 4.76, 5.56 and 7.91 are presented in figure 14. These signatures were obtained to provide a base for comparing the signatures obtained from the model with the various simulated plumes. The data were obtained at altitude-to-model length ratios of approximately .5. This small distance will not produce any inaccuracies in the extrapolations since the model is a body of revolution. The length used in the ratio h/ℓ in this and all subsequent figures is the model length without escape tower and engines (see figure 2).

The pressure signatures obtained from tests of the .00337-scale Saturn model with the 2/3-inviscid boundary simulated plume is shown in figure 15. The data of figures 16 and 17 are for the .00337-scale model with inviscid-boundary plume and the .00168-scale model with mixing boundary plume, respectively.

Most of the pressure signature data for the hypersonic Mach numbers exhibit overpressures too large to be extrapolated by by the weak wave method of reference 1 and hence the technique discussed above in connection with the Apollo command module data must be employed. This technique is discussed in the Appendix.

REFERENCES

1. Thomas, Charles L.: Extrapolation of Wind Tunnel Sonic Boom Signatures Without Use of a Whitham F-Function. NASA SP-255, 1971.

2. Hicks, Raymond M.; Mendoza, Joel P.; and Garcia, Frank Jr.: A Wind Tunnel-Flight Correlation of Apollo 15 Sonic Boom. NASA TM X-62,111, January 28, 1972.

3. Hicks, Raymond M.; and Mendoza, Joel P.: Prediction of Aircraft Sonic Boom Characteristics From Experimental Near Field Results. NASA TM X-1477, 1967.

4. Hicks, Raymond M.; Mendoza, Joel P.; and Hunton, Lynn W.: Some Effects of Mach Number and Geometry on Sonic Boom. NASA TN D-4214, October 1967.

APPENDIX

EXTRAPOLATION OF PRESSURE SIGNATURES

RESULTING FROM STRONG SHOCK WAVES

Existing methods for extrapolating near field sonic boom pressure signatures assume (1) that the propagation speed (u+a) of each waveform point can be calculated by linearized, isentropic theory, (2) that shock propagation speeds are equal to the average value of (u+a) across the shock, (3) that all propagation velocities are directed normal to the free stream Mach cone, and (4) that the pressure disturbance, Δp, of each waveform point varies as $1/\sqrt{h}$. These assumptions are justifiable only if the near field signature is weak $\left(\frac{\Delta p}{p} < .5\right)$. However, as illustrated in this report, a strong near field signature is obtained when the flight vehicle is nonslender and the signature is measured close to the body. In order to extrapolate strong pressure signatures it is necessary to avoid using the above four assumptions. This can be accomplished as described below.

Instead of using linearized isentropic theory to calculate the propagation speed (u+a) of each waveform point, the normal shock relations should be used to calculate $\Delta(u+a)$ across each shock along with the full isentropic expressions to calculate the variation of (u+a) between shocks. The pertinent normal shock relations are:

$$u_2 = u_1 + \frac{a_1}{\gamma}\left(\frac{p_2}{p_1} - 1\right)\left[\frac{\frac{2\gamma}{\gamma+1}}{\frac{p_2}{p_1} + \frac{\gamma-1}{\gamma+1}}\right]^{1/2}$$

$$a_2 = a_1\left[\frac{\frac{p_2}{p_1}\;\frac{\frac{\gamma+1}{\gamma-1} + \frac{p_2}{p_1}}{1 + \frac{\gamma+1}{\gamma-1}\frac{p_2}{p_1}}}\right]^{1/2}$$

where p_1, a_1, and u_1 are the values of absolute pressure, sound speed, and fluid particle speed, respectively, just ahead of the shock and p_2, a_2 and u_2 are the values just behind the shock. The full isentropic relations for determining the variation of (u+a) between shocks are:

$$u = u_r + \frac{2a_r}{\gamma - 1}\left[\left(\frac{p}{p_r}\right)^{\frac{\gamma - 1}{2\gamma}} - 1\right]$$

$$a = a_r\left(\frac{p}{p_r}\right)^{\frac{\gamma - 1}{2\gamma}}$$

where p_r, a_r, and u_r are reference values of p, a, and u, which should be taken to be the values of p_2, a_2, and u_2 corresponding to the last shock crossed.

Shock propagation speeds (relative to the undisturbed fluid) should be calculated using

$$U_s = u_1 + a_1\left(\frac{\gamma-1}{2\gamma} + \frac{\gamma+1}{2\gamma}\frac{p_2}{p_1}\right)^{1/2}$$

rather than the equation for the average value of (u+a) across the shock.

All propagation velocities should be directed normal to the front shock, rather than normal to the free stream Mach cone. The wave angle, θ, of the front shock can be calculated from

$$\sin\theta = \left[\frac{(\gamma-1) + (\gamma+1)\frac{p_2}{p_1}}{2\gamma M_\infty^2}\right]^{1/2}$$

The assumption that all propagation velocities are directed normal to the front shock is probably invalid for aft portions of the signature, if the signature is very strong. It is therefore recommended that only the front (positive) portion of the signature be extrapolated.

The final modification is in regard to the attenuation due to wavefront spreading. The weak wave assumption that the perturbation pressure varies as $1/\sqrt{h}$ is a result of conservation of kinetic energy, $\rho u^2 h$, for each waveform point. For a weak wave, u is proportional to the perturbation pressure, Δp, and the density is very nearly constant. However, if the wave is strong, the density variation should be accounted for, as well as the nonlinear dependence of u on Δp. Assuming that the full isentropic expression for u(p) can be applied throughout the signature, with $p_r = p_\infty$, the relationship between Δp and h is found to be

$$\left(1 + \frac{\Delta p}{p_\infty}\right)^{1/2} - \left(1 + \frac{\Delta p}{p_\infty}\right)^{1/2\gamma} = \frac{\text{const.}}{\sqrt{h}}$$

The above strong wave treatment represents an extremely simplified view of a complex flow field. However, extrapolations based upon these considerations should provide more accurate results than would be obtained by using weak wave assumptions when the signature is strong. When the signature is weak, the strong wave relations reduce exactly to those used previously for weak waves.

A comparison of extrapolations of a strong near field signature using a strong wave extrapolation program and a weak wave extrapolation program are shown in figure 18. The experimental signatures were obtained in the Ames 61 m. Pressurized Ballistic Range. It is seen that the strong wave extrapolation program provides a more accurate prediction of the signature at h/d = 14.3 than does the weak wave extrapolation program. This ballistic-range data are currently the only experimental results available for verifying the strong wave extrapolation technique. A wind tunnel verification is needed, in order to avoid the reflection factor problem discussed below.

In a ballistic range, pressure signatures are measured using a microphone mounted in a flat plate. Therefore, each signature must be divided by the correct reflection factor before extrapolation so as to obtain the correct propagation speeds. The reflection factor of the front shock of the signature can be easily determined from oblique shock theory and results are shown in figure 19. When the overpressures are small the entire signature is scaled by the reflection factor. However, when the overpressures are large it is questionable whether the reflection factor is constant over the signature length. It is possible that some parts of the signature should be scaled differently from others. Until this uncertainty is experimentally resolved, the reflection factor for data obtained in ballistic ranges will have to be applied to signatures with large values of overpressure in the same manner as it is applied to signatures with small values of overpressure. The extrapolations of figure 18 were based upon a reflection factor of 2.9, with the exception of the dashed signature, which is included to illustrate the difference that results from incorrectly using a reflection factor of two (the reflection factor for a weak wave).

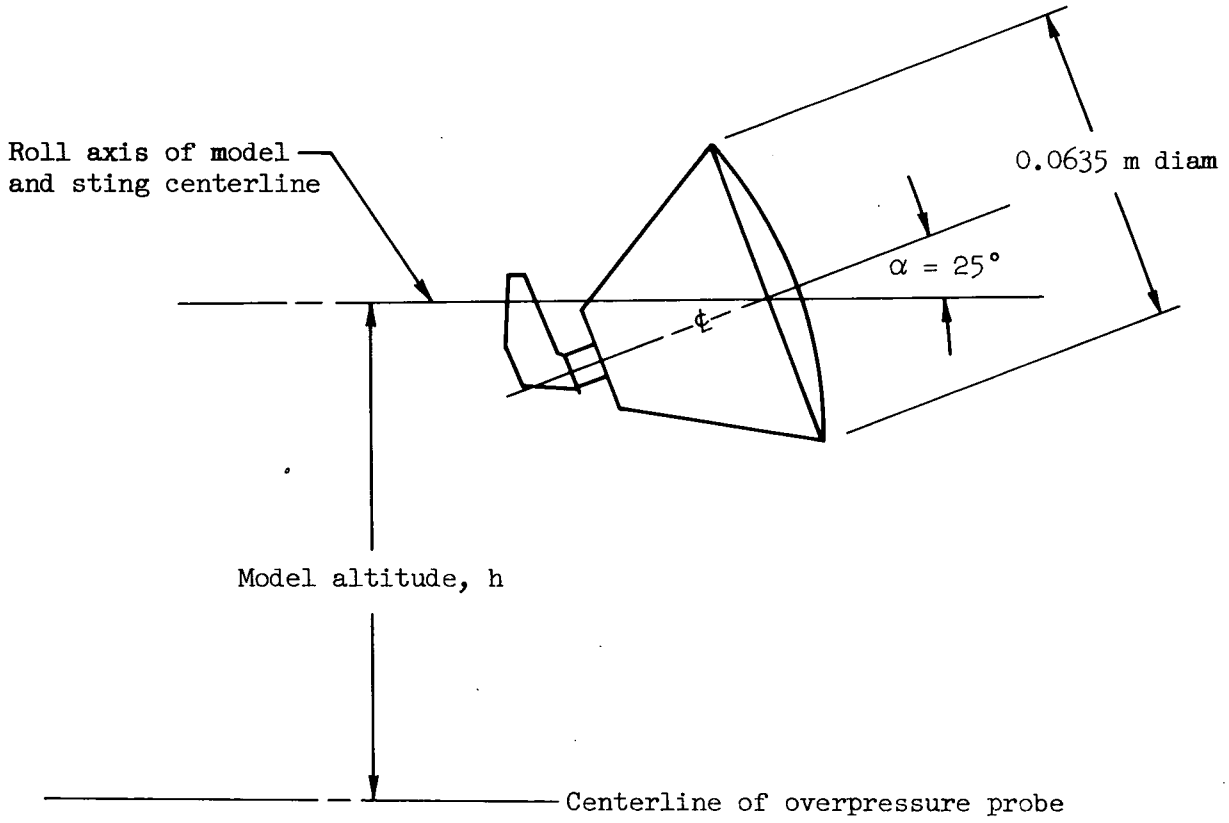

Figure 1.- 0.016-scale model of the Apollo command module; $\alpha = 25°$, $\Phi = 0°$.

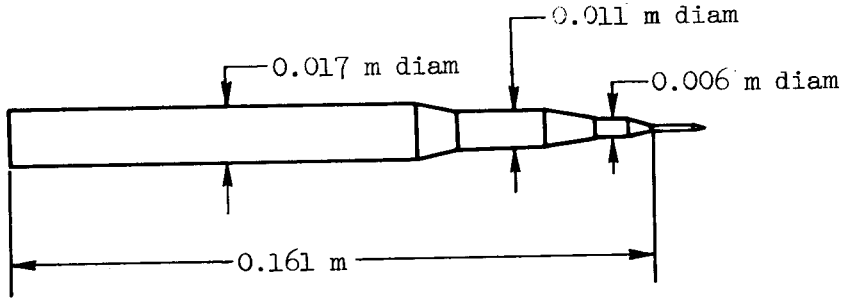

(a) 0.00168-scale model

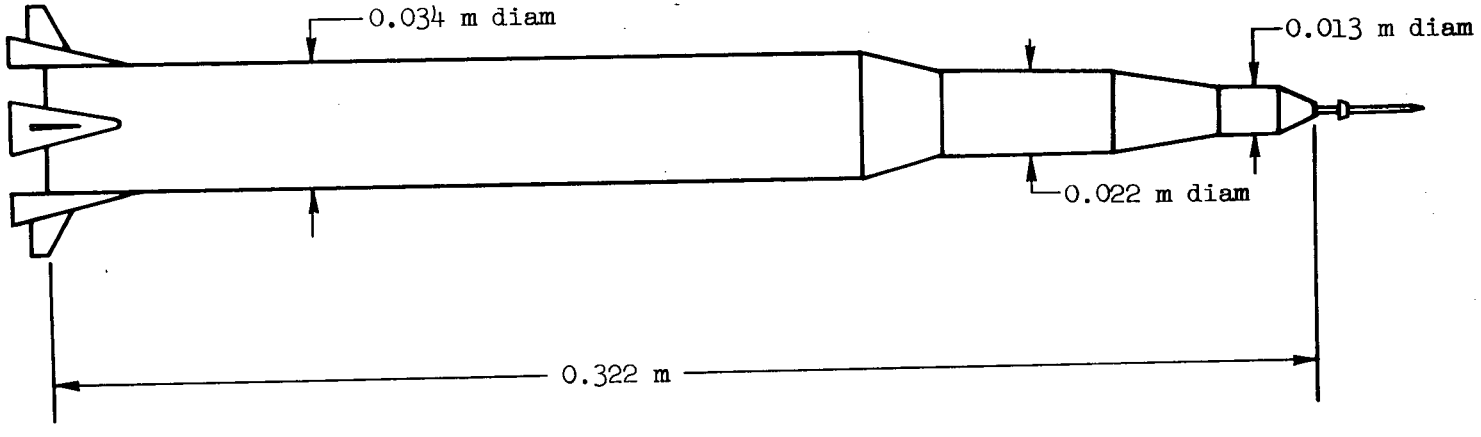

(b) 0.00337 scale model

Figure 2.- Saturn test models.

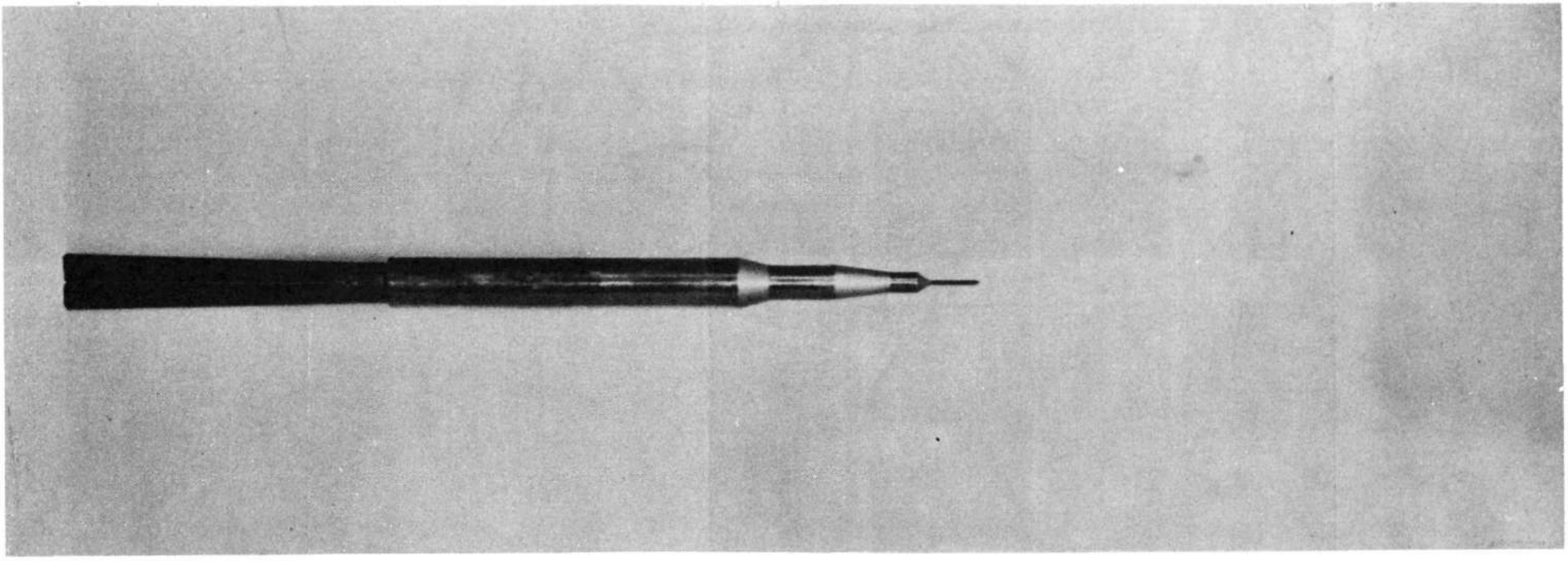

(a) 0.00168-scale model

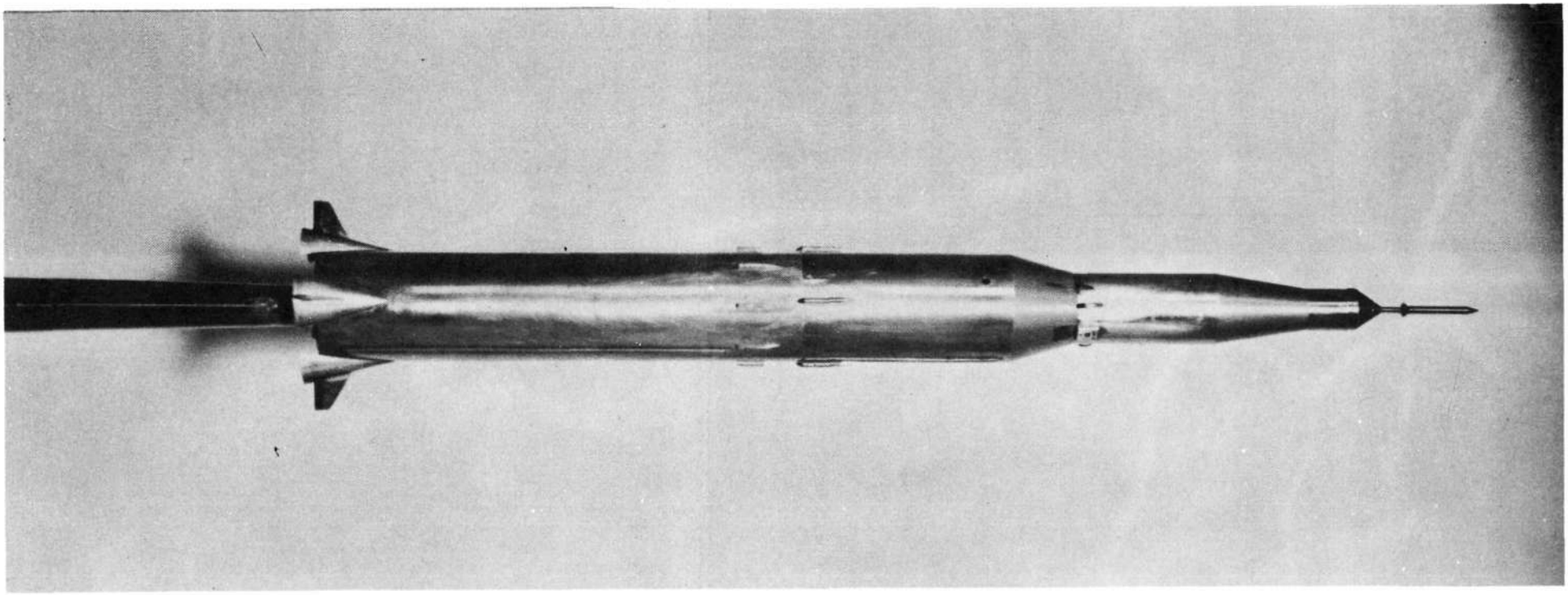

(b) 0.00337-scale model

Figure 3.- Model photographs.

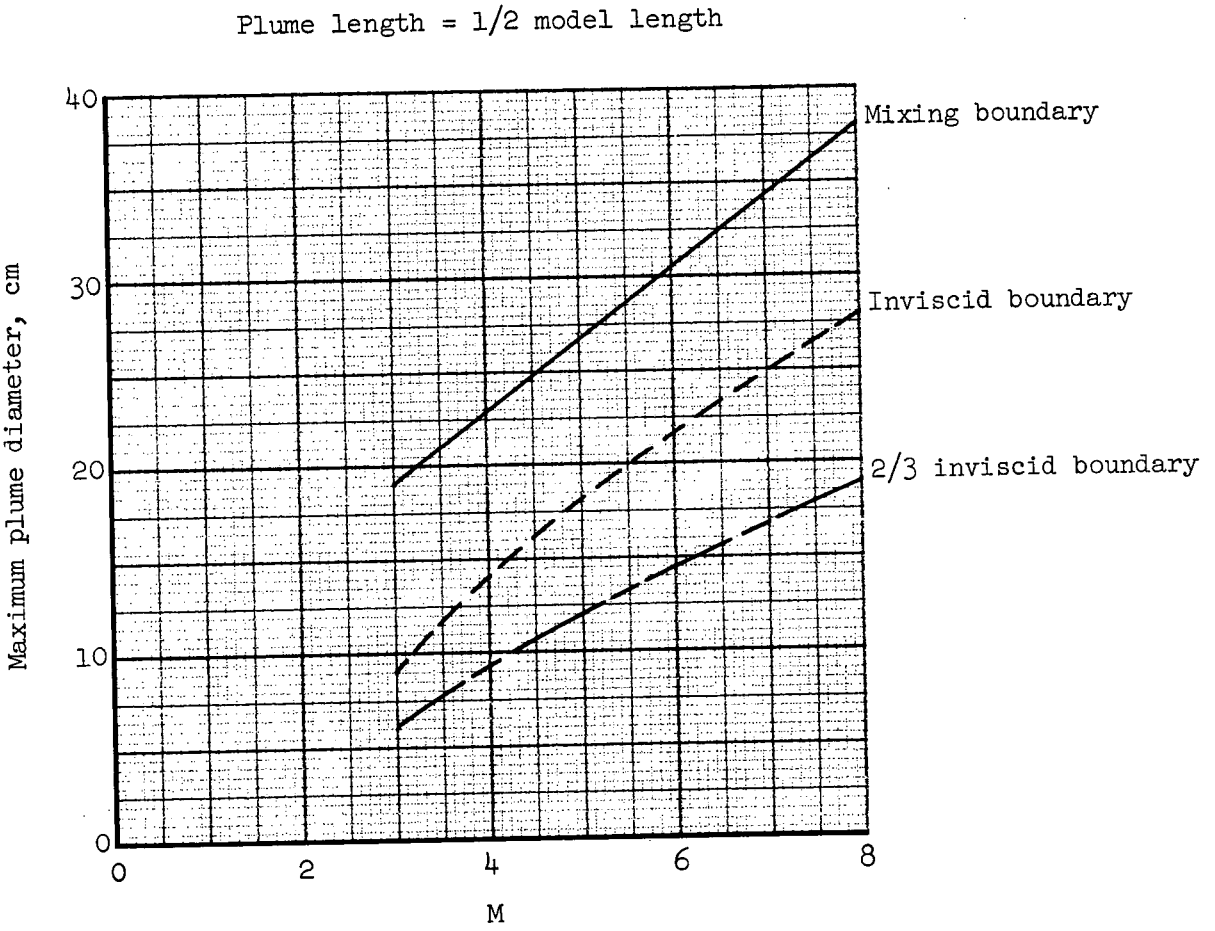

Figure 4.- Diameter of simulated plumes.

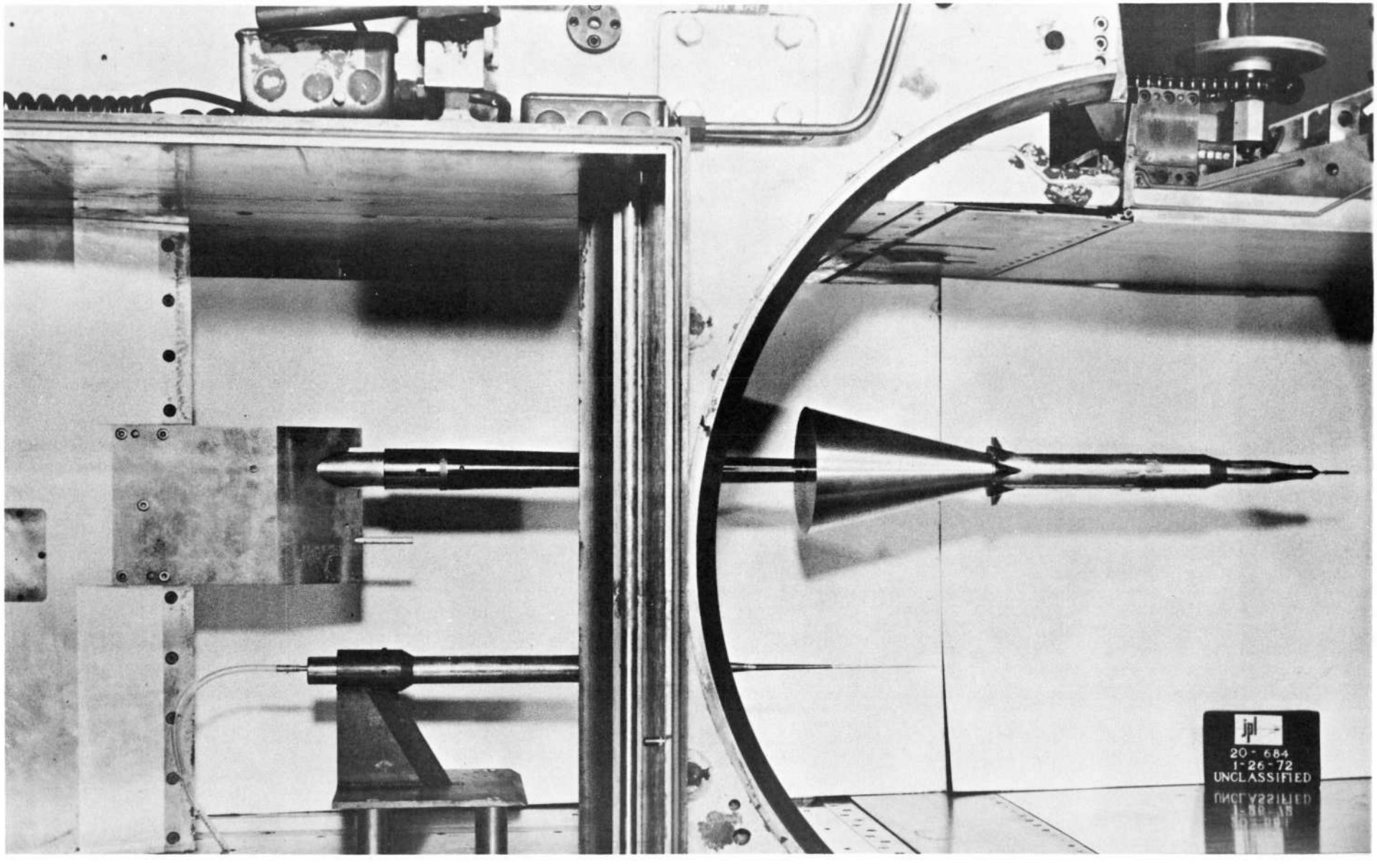

Figure 5.- Large model with simulated plume installed in JPL 20-Inch Supersonic Wind Tunnel.

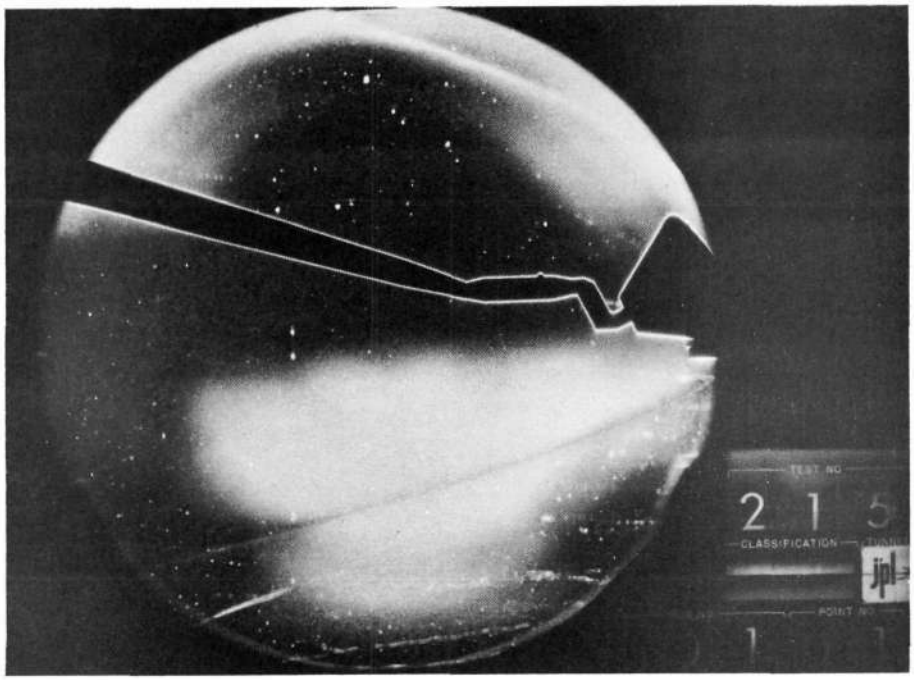

(a) $\varphi = 0°$

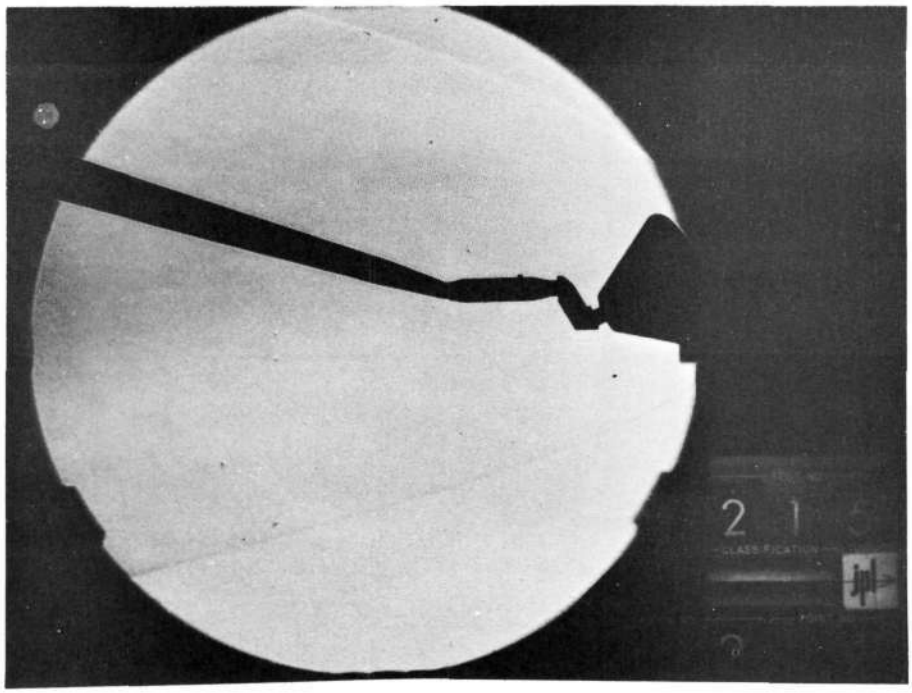

(b) $\varphi = 30°$

Figure 6.- Schlieren photographs of the Apollo command module; M = 10.1, $\alpha = 25°$.

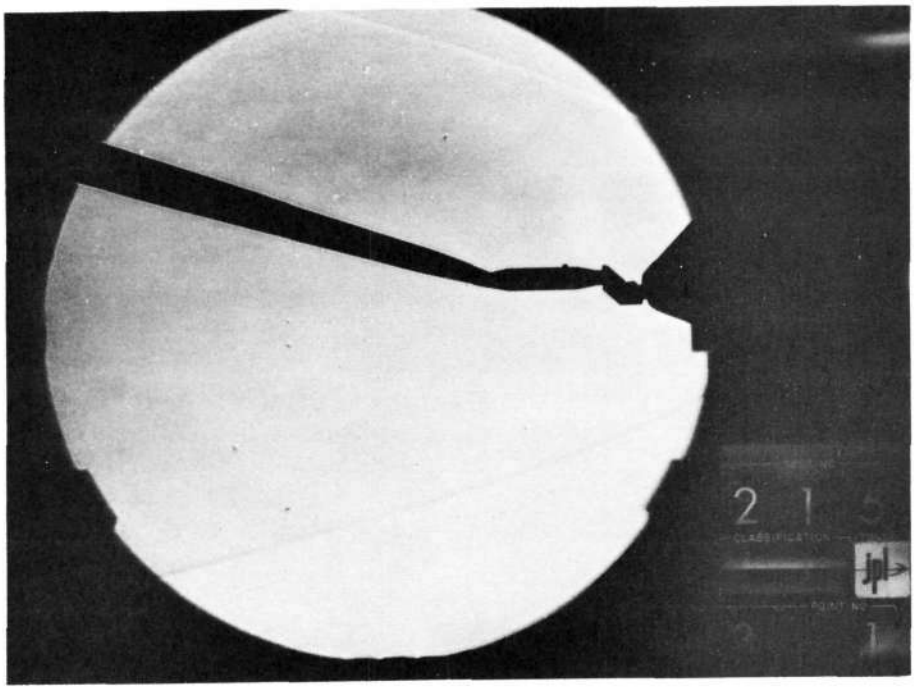

(c) $\varphi_1 = 60°$

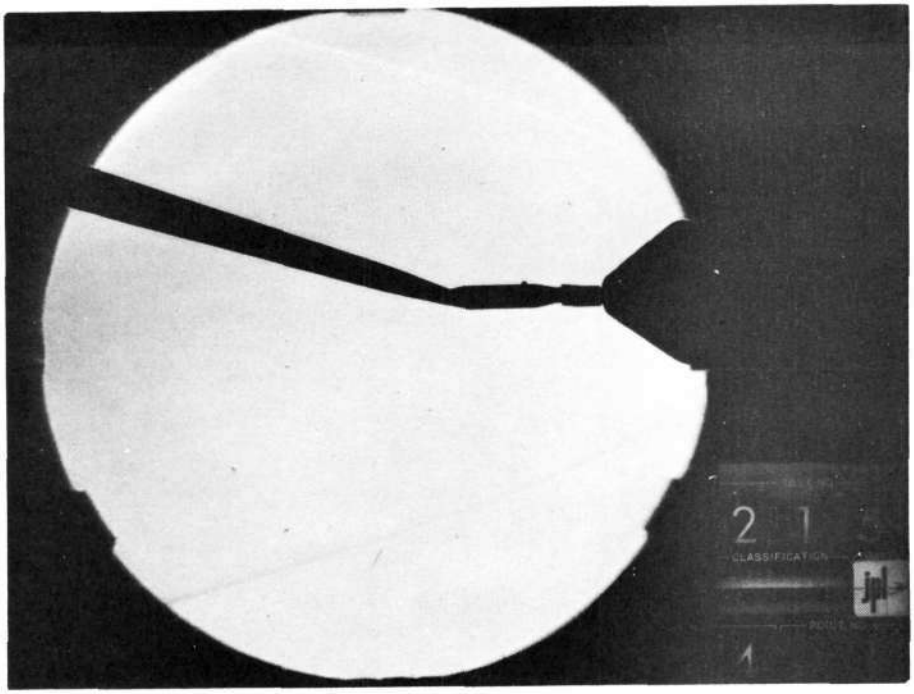

(d) $\varphi_1 = 90°$

Figure 6.- Continued.

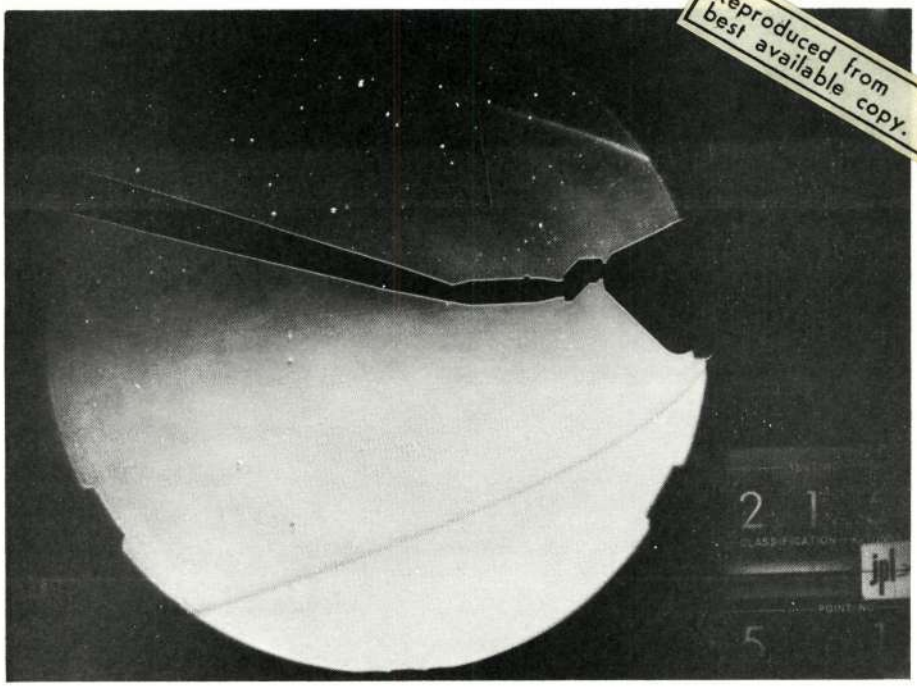

(e) $\varphi = 120°$

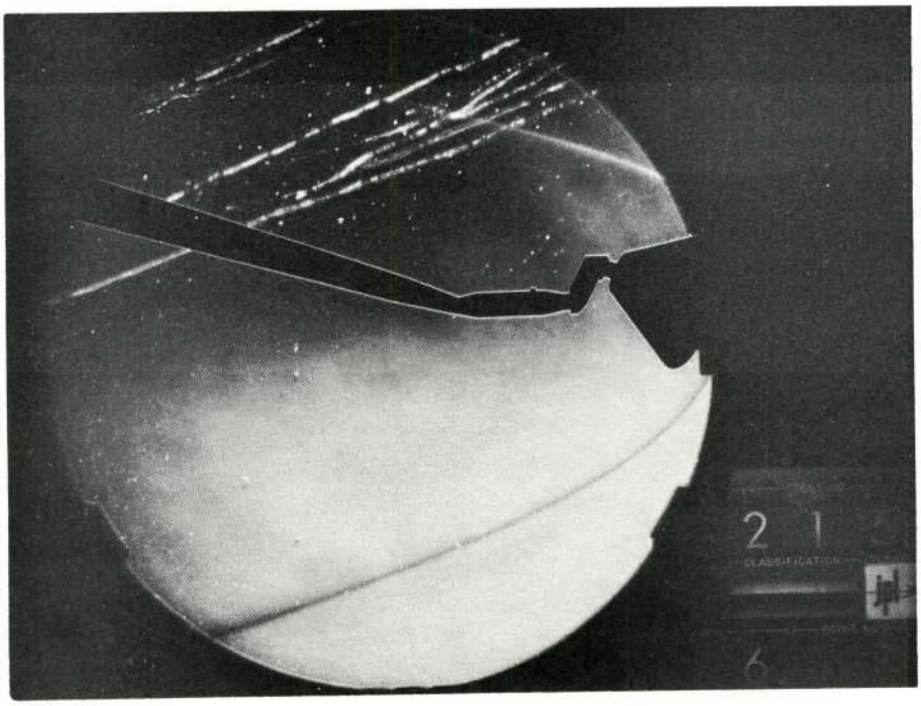

(f) $\varphi = 150°$

Figure 6.- Continued.

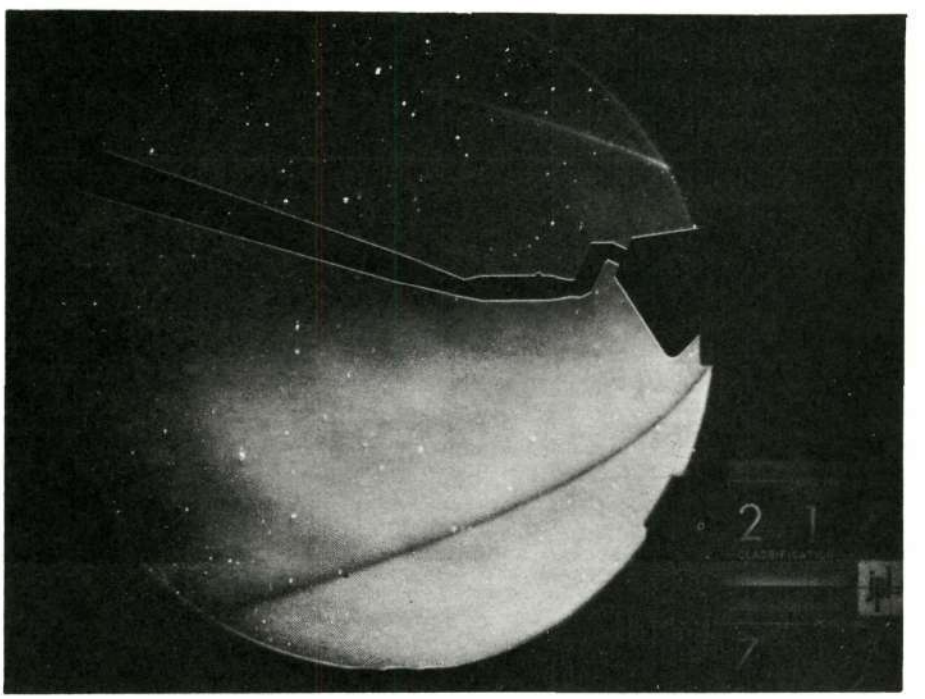

(g) $\varphi = 180°$

Figure 6.- Concluded.

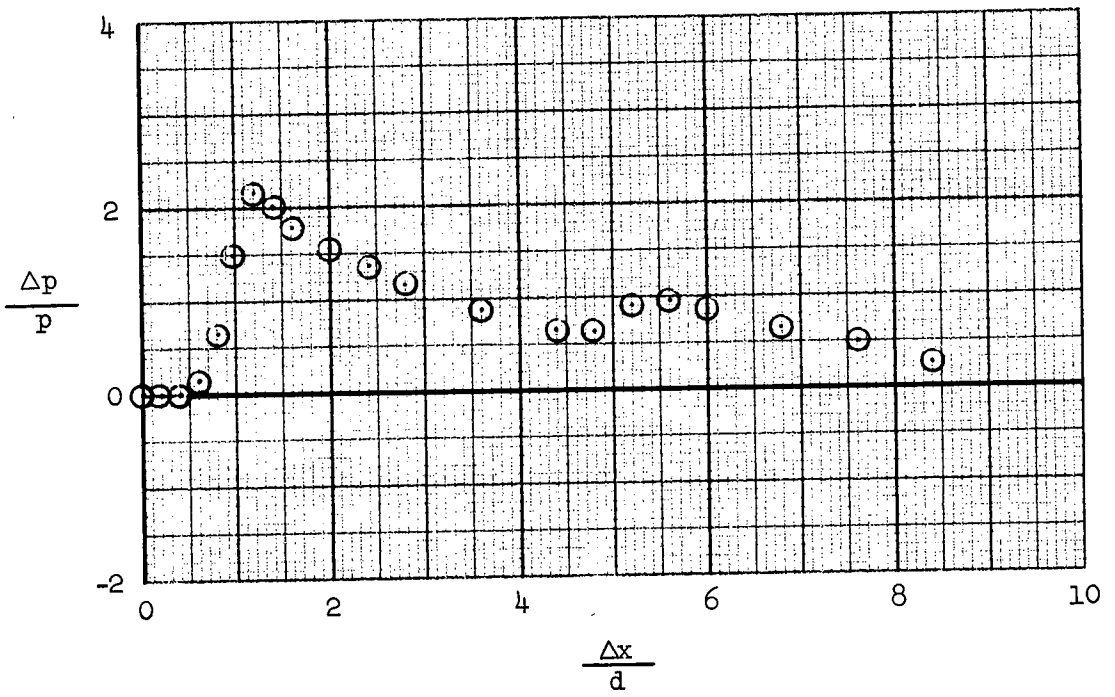

(a) $\varphi = 0°$

Figure 7.- Wind tunnel pressure signatures for the Apollo command module; M = 10.1, $\alpha = 25°$, h/d = 2.85.

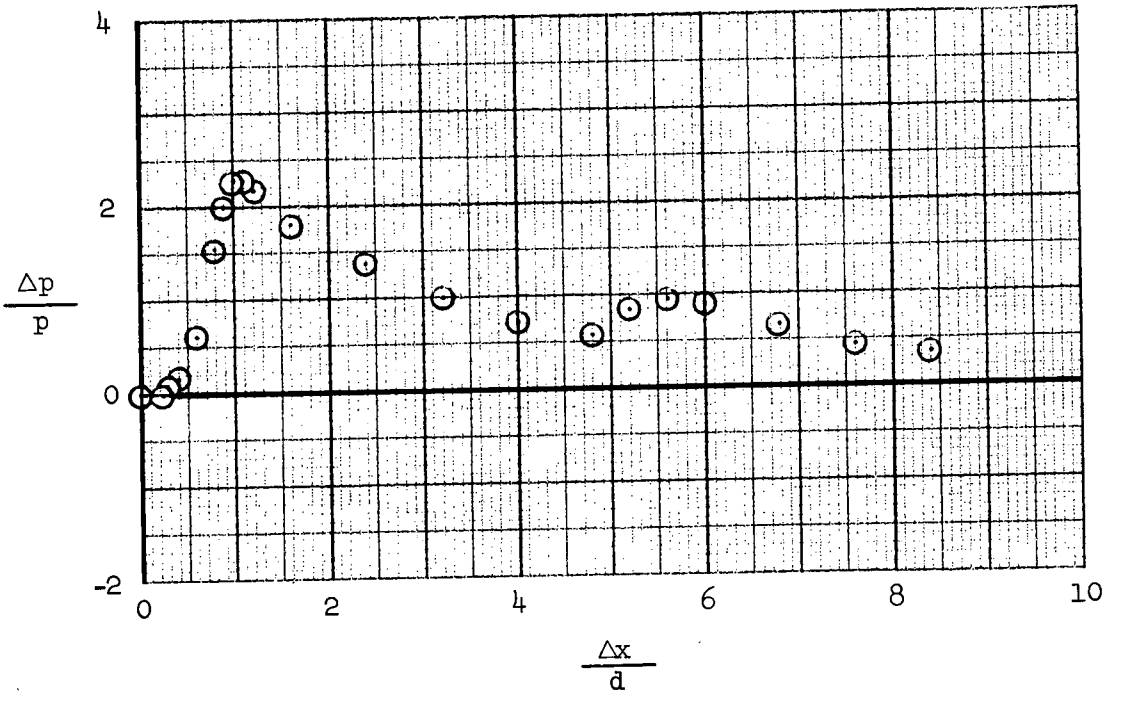

(b) $\varphi = 30°$

Figure 7.- Continued.

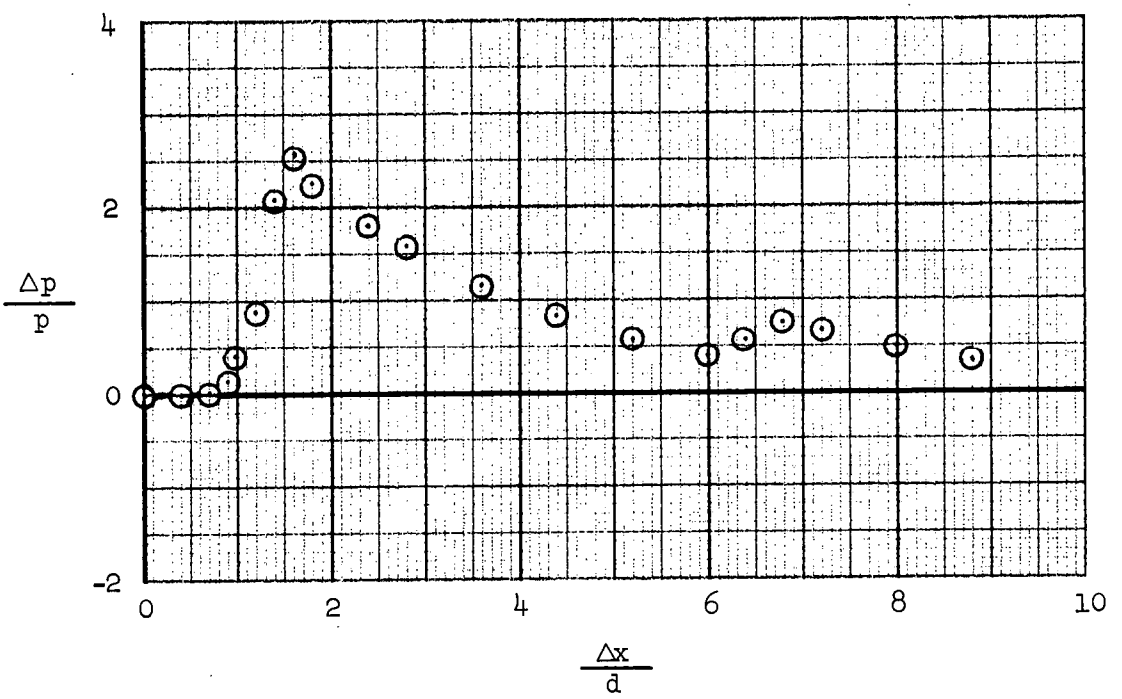

(c) $\varphi = 60°$

Figure 7.- Continued.

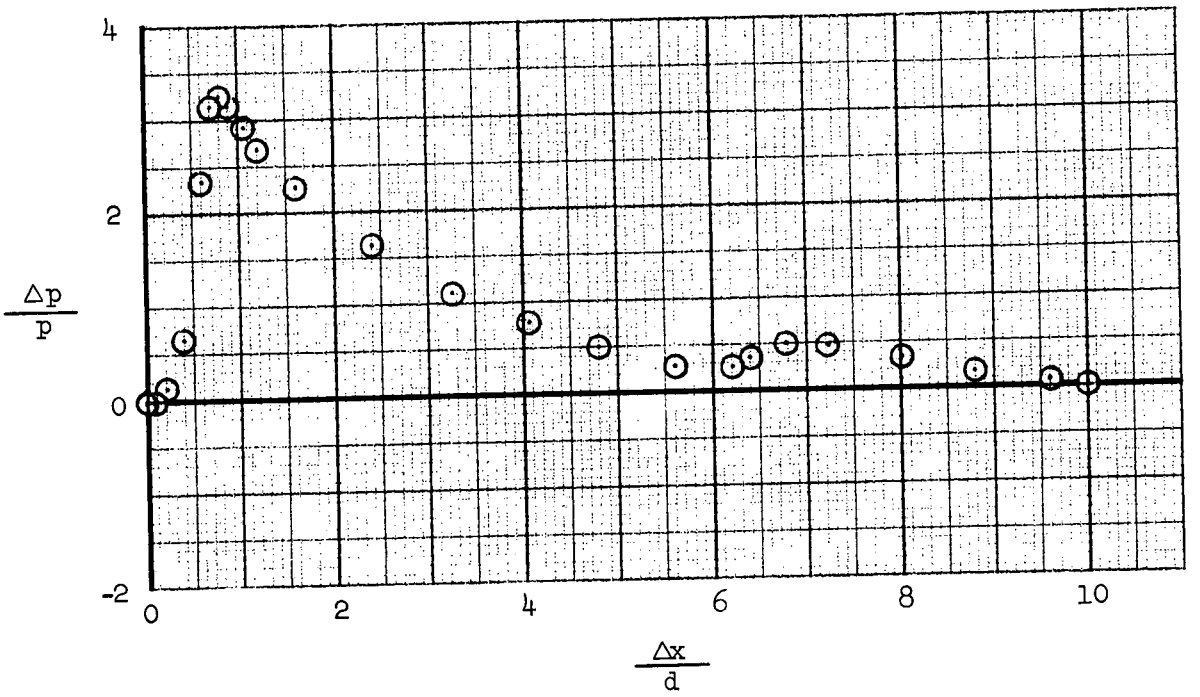

(d) $\varphi = 90°$

Figure 7.- Continued.

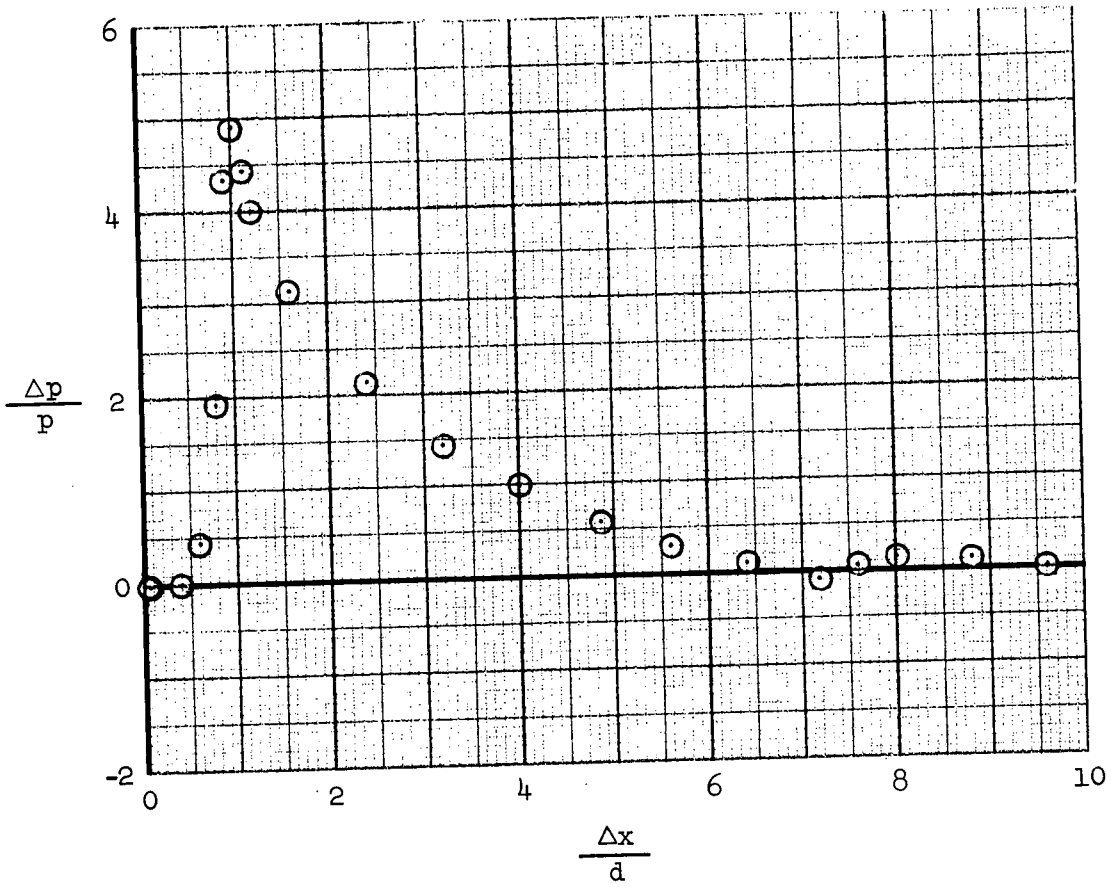

(e) $\varphi = 120°$

Figure 7.- Continued.

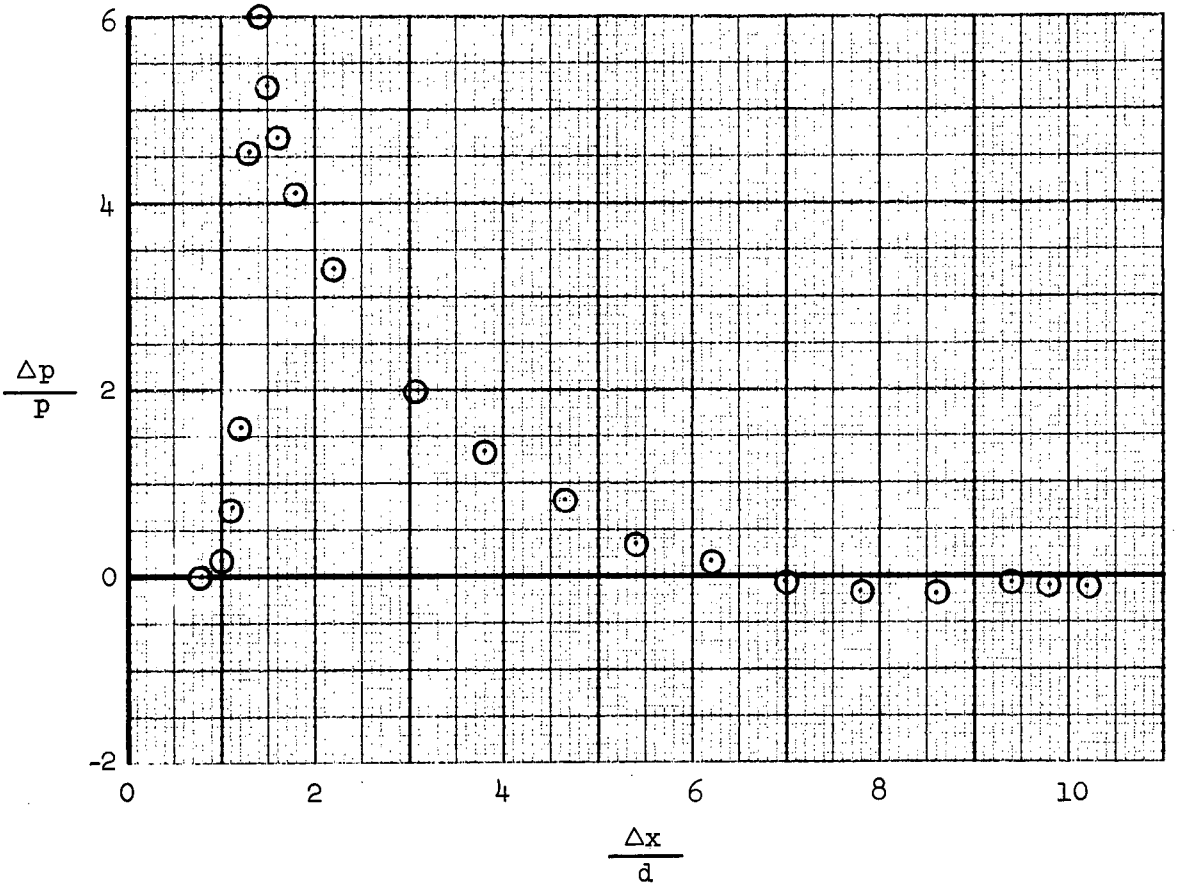

(f) $\varphi = 150°$

Figure 7.- Continued.

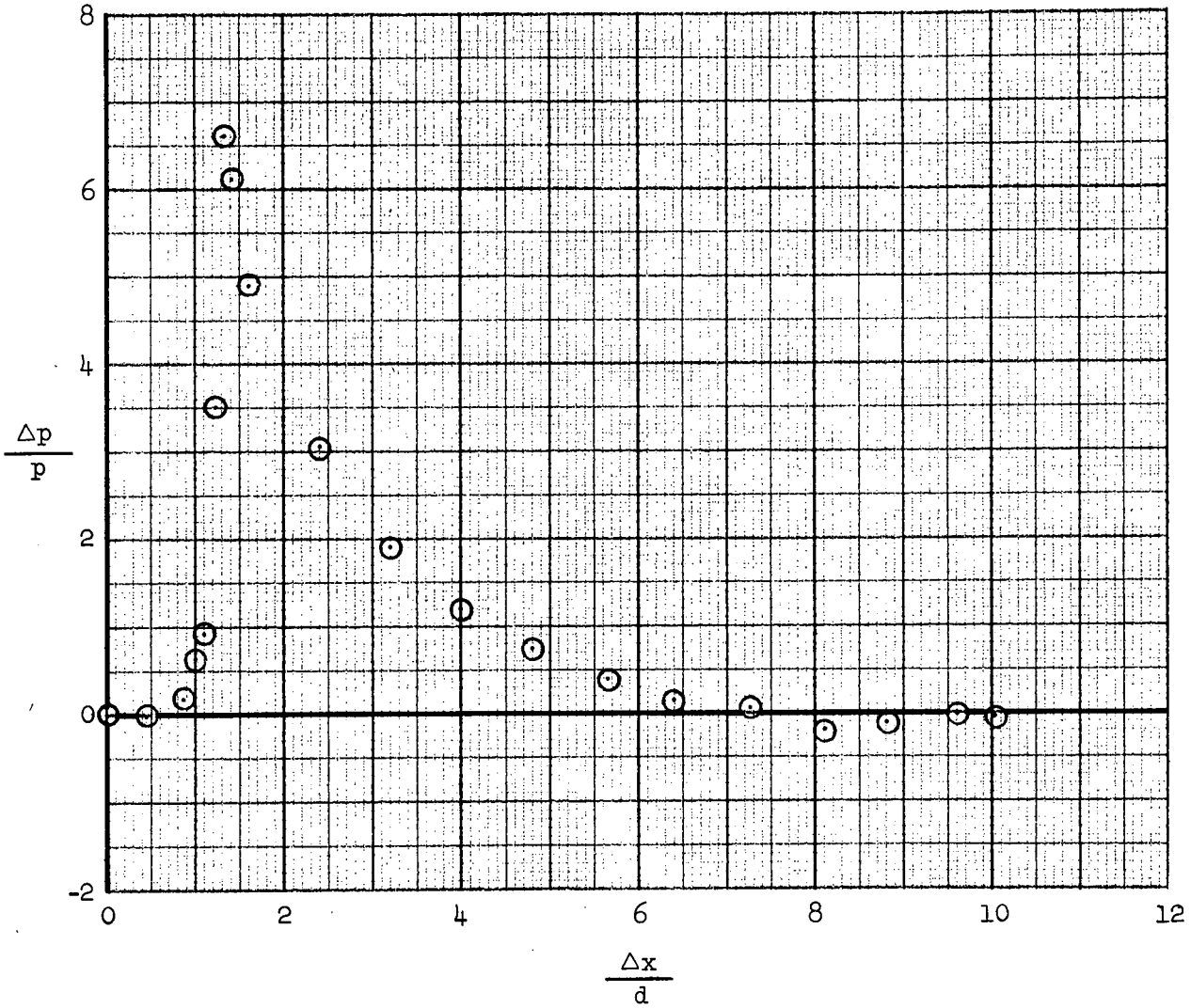

(g) $\varphi = 180°$

Figure 7.- Concluded.

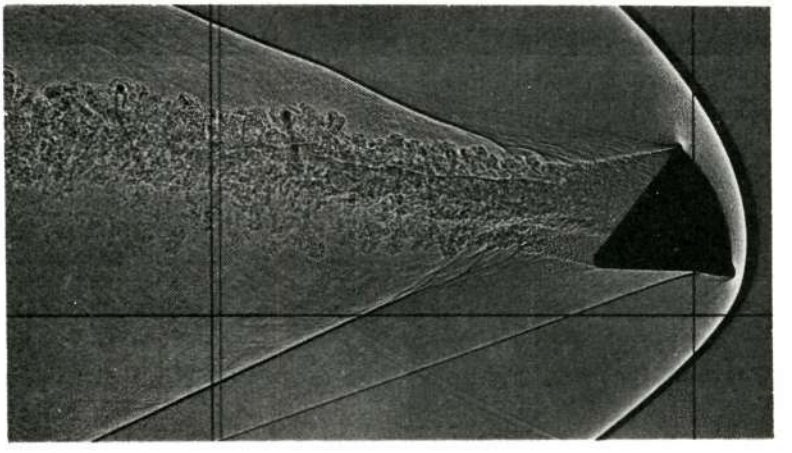

Figure 8.- Shadowgraph taken in Ames 200-Foot Pressurized Ballistic Range; $M = 2.2$, $\alpha = 25°$.

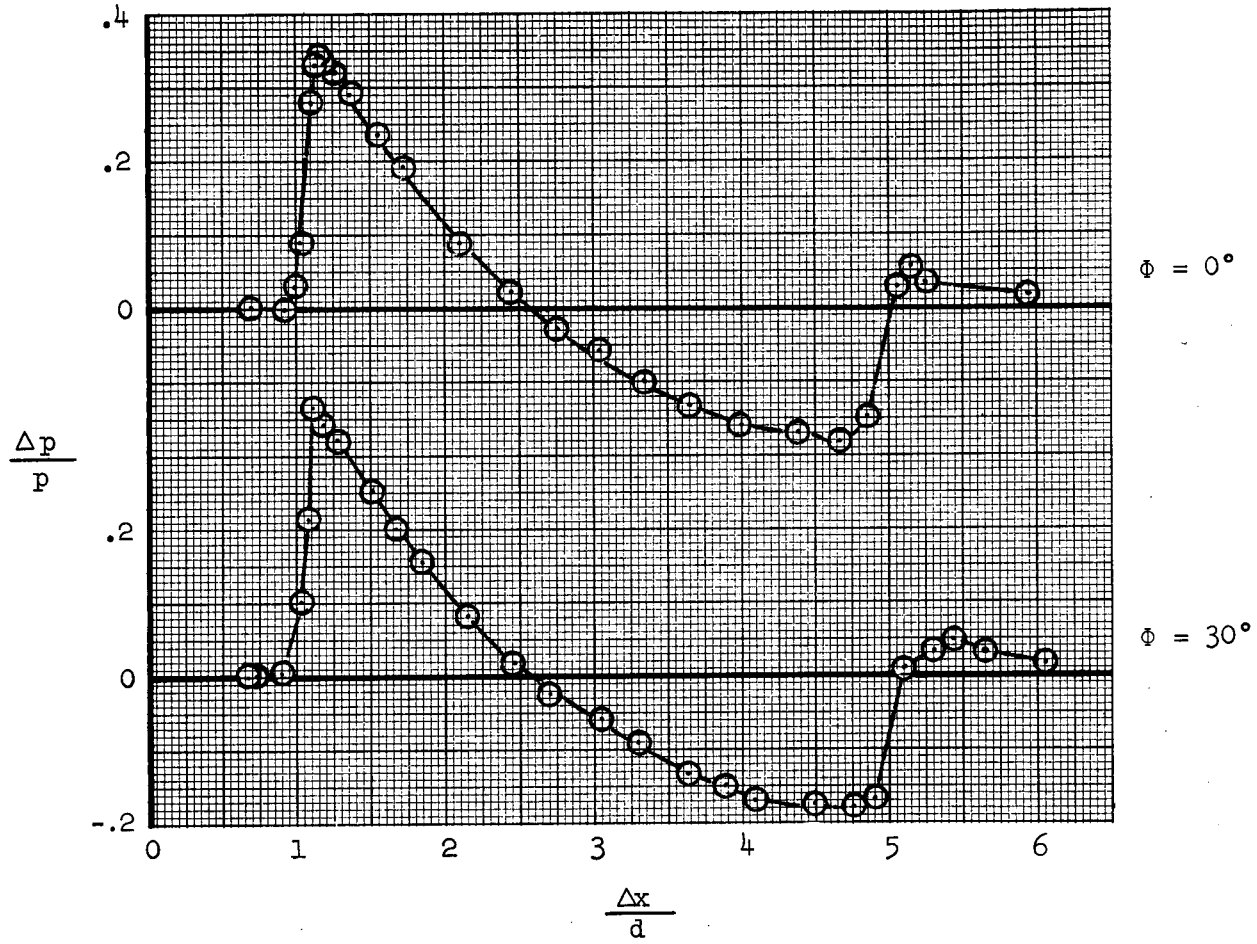

Figure 9.- Wind tunnel pressure signatures for the Apollo command module; M = 2.0, α = 25°, φ = 0° and 30°, h/d = 2.85.

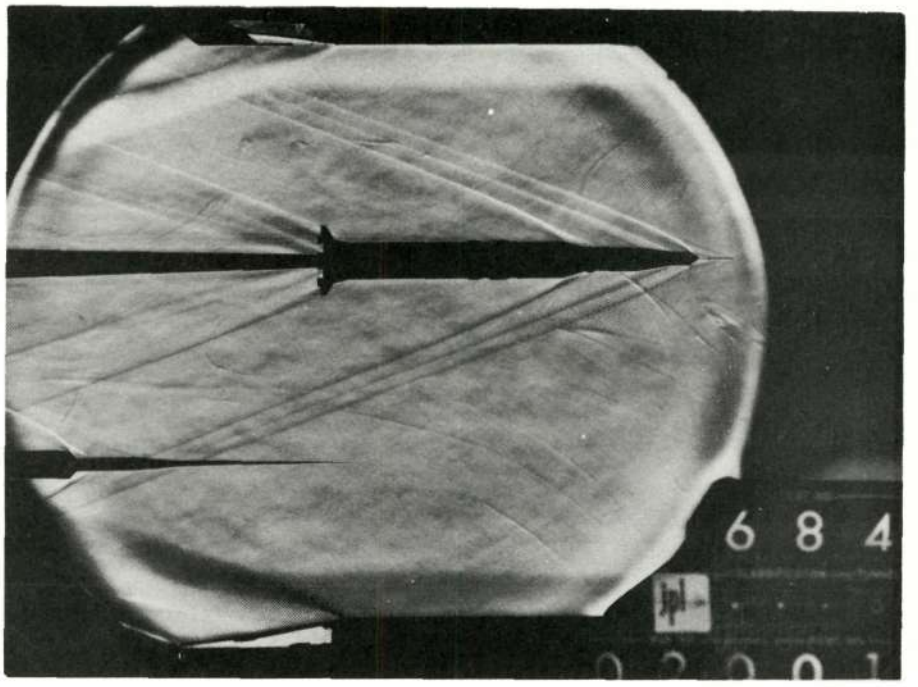

(a) M = 3.01

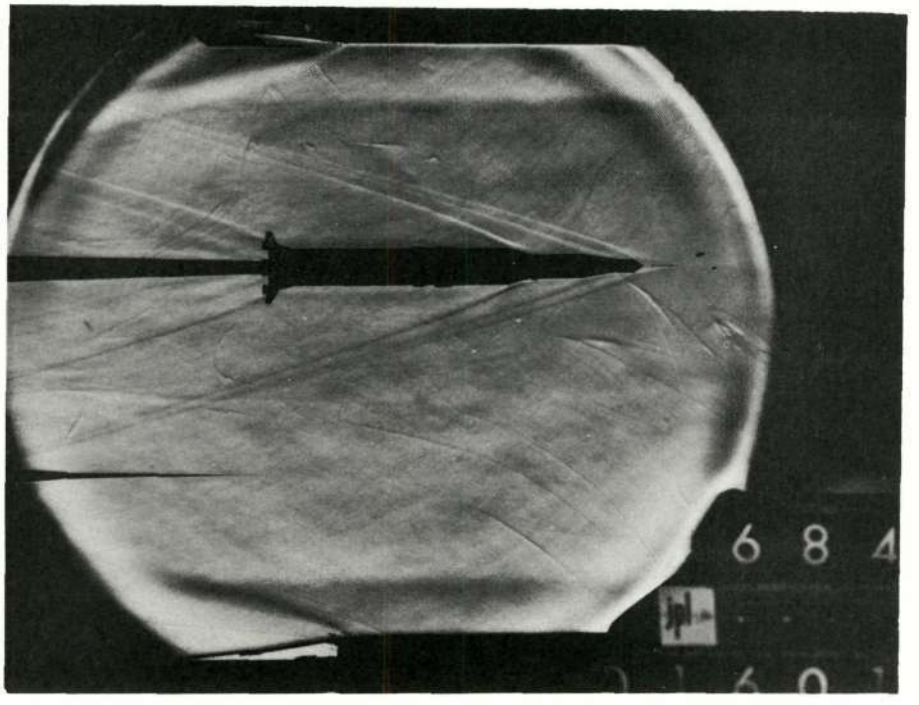

(b) M = 3.98

Figure 10.- Shadowgraphs of 0.00337-scale Saturn model; no plume, $\alpha = 0°$.

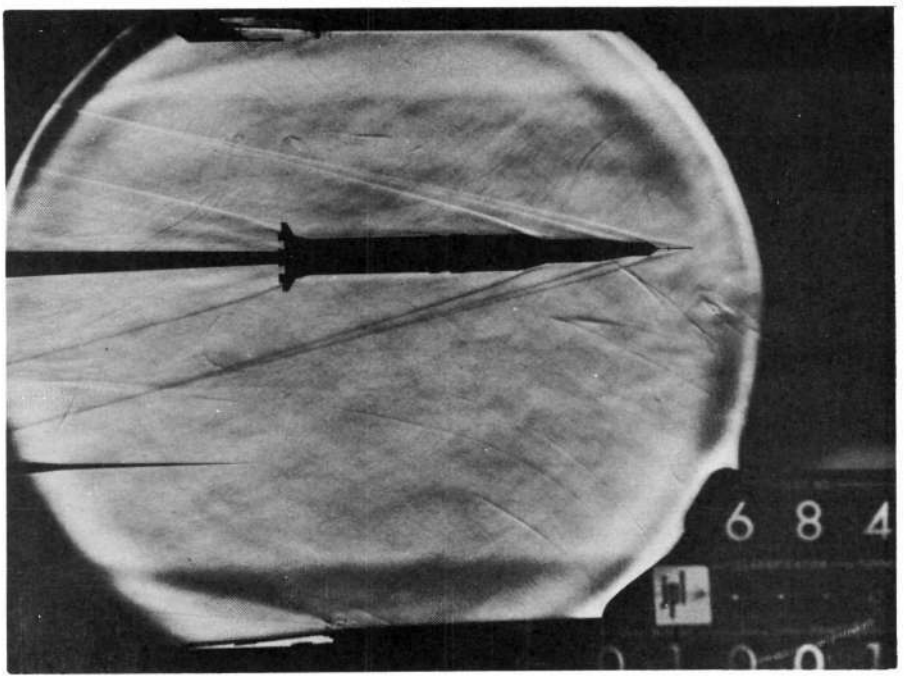

(c) M = 4.76

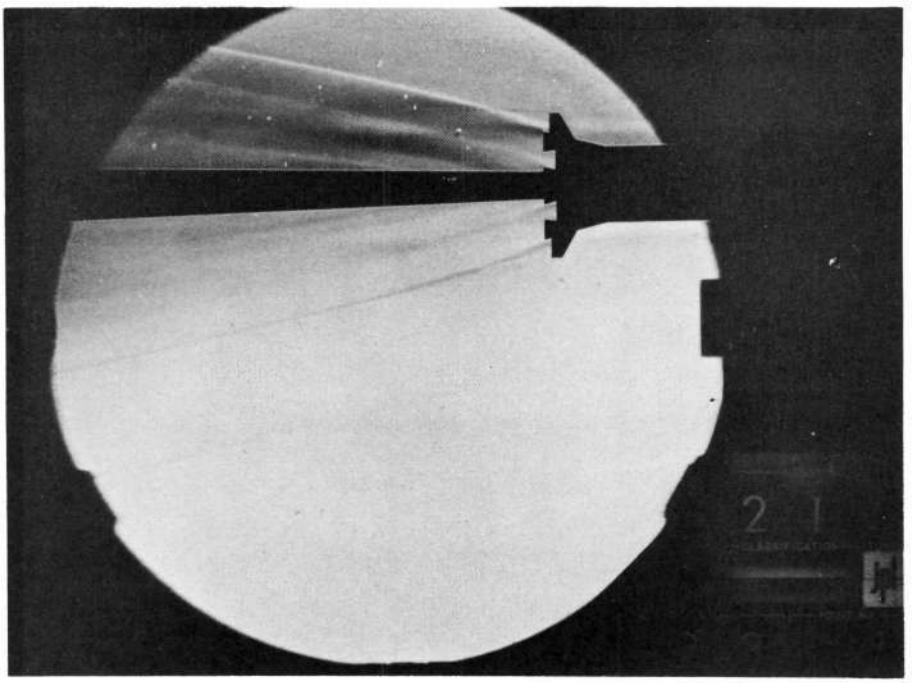

(d) M = 5.56

Figure 10.- Continued.

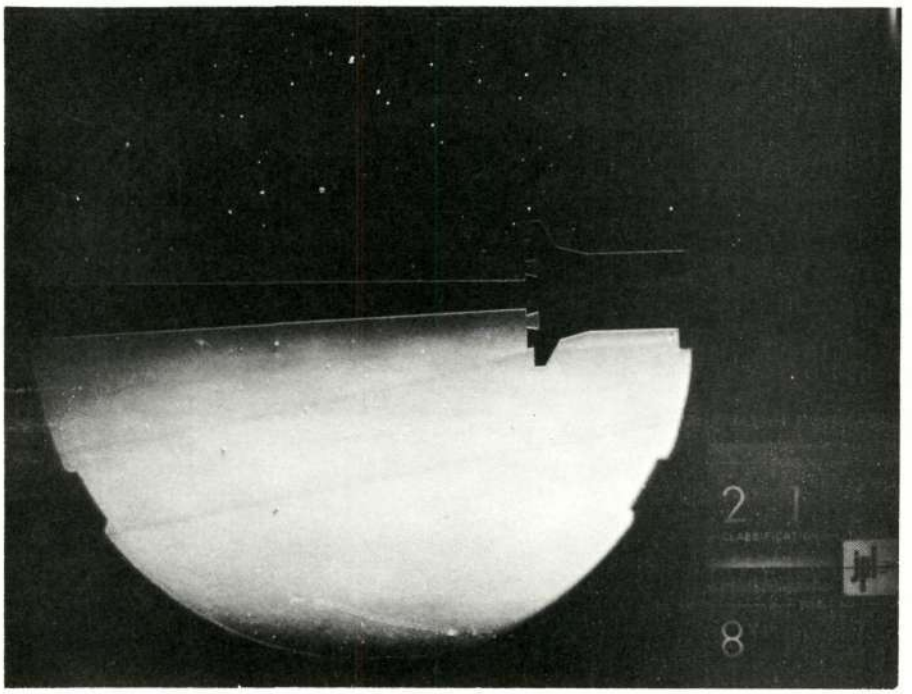

(e) M = 7.91

Figure 10.- Concluded.

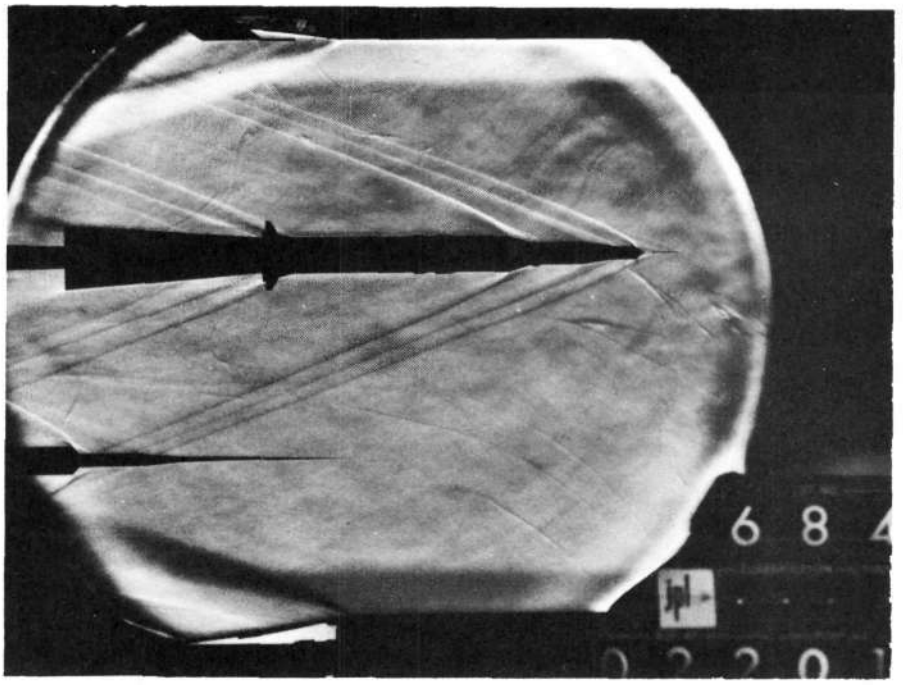

(a) M = 3.01

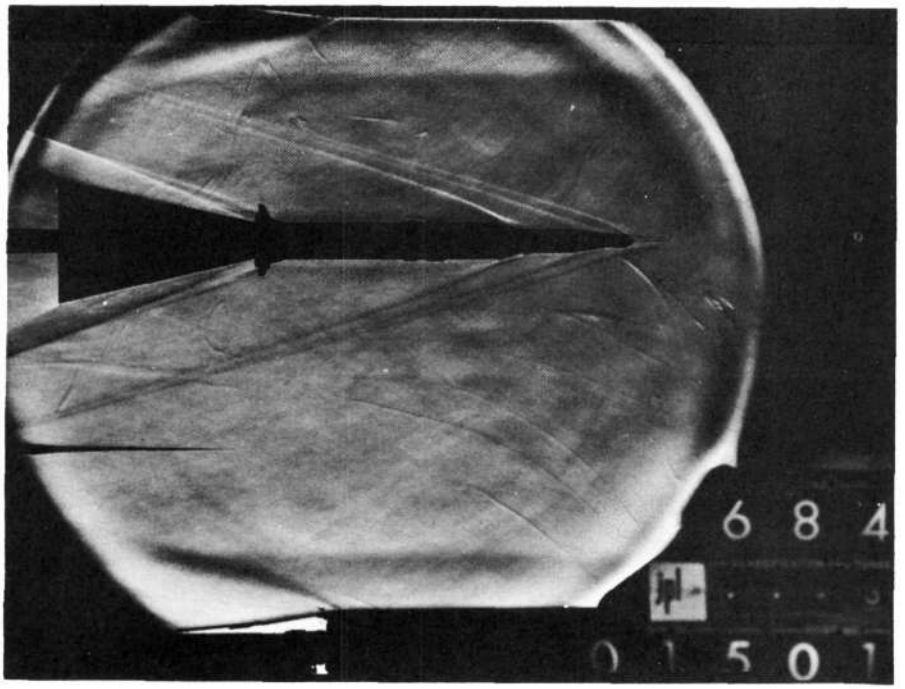

(b) M = 3.98

Figure 11.- Shadowgraphs of 0.00337-scale Saturn model, 2/3 inviscid boundary, plume; $\alpha = 0°$.

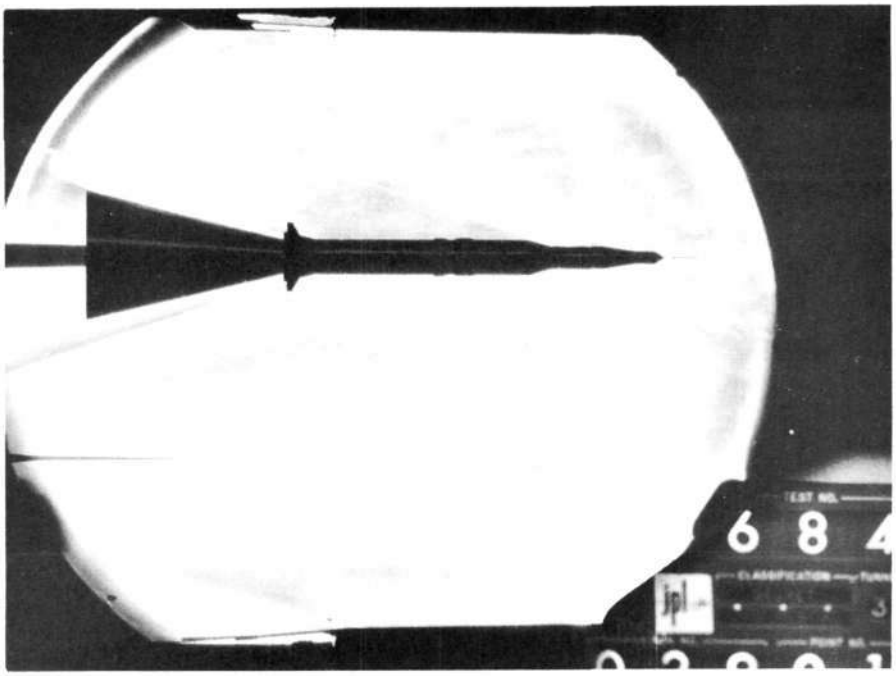

(c) M = 4.76

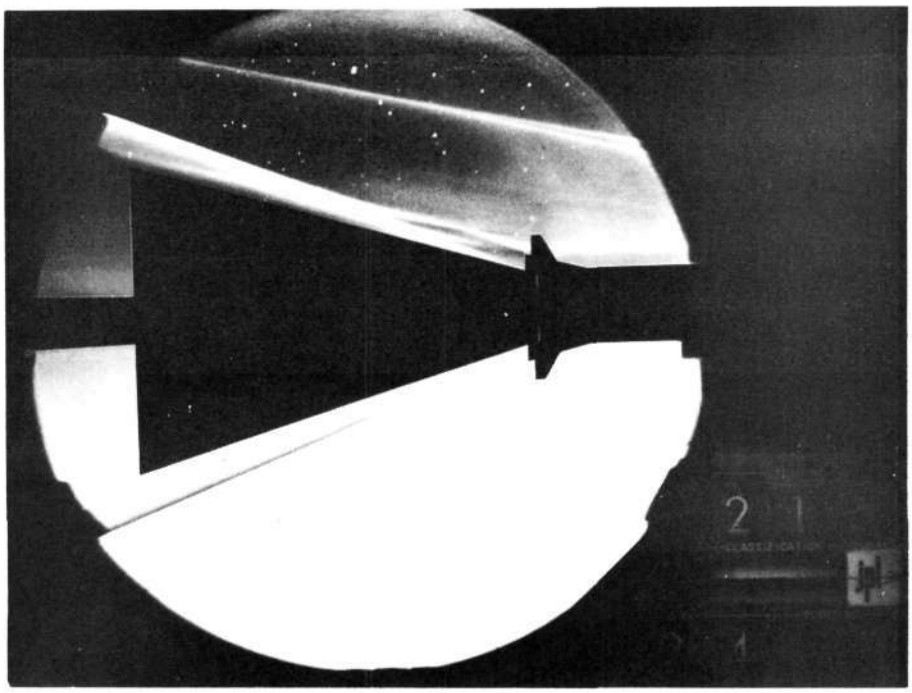

(d) M = 5.56

Figure 11.- Concluded.

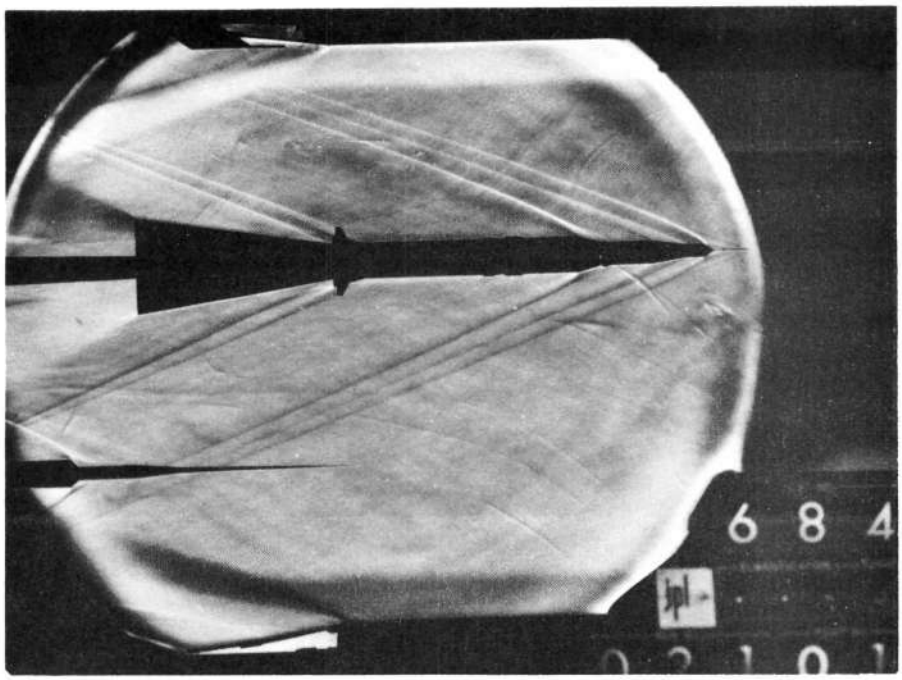

(a) M = 3.01

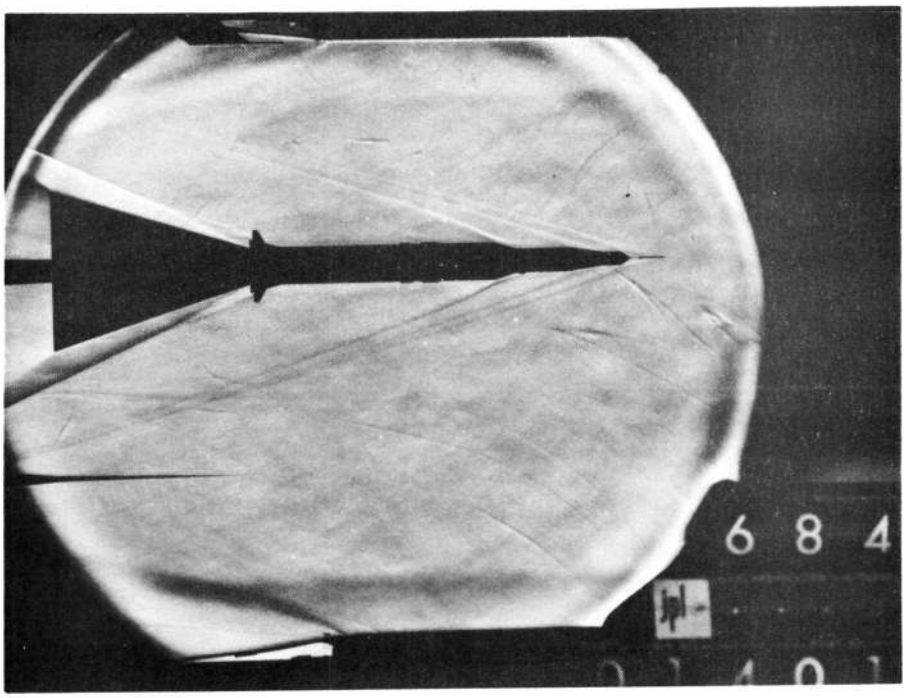

(b) M = 3.98

Figure 12.- Shadowgraphs of 0.00337-scale Saturn model, inviscid boundary, plume; $\alpha = 0°$.

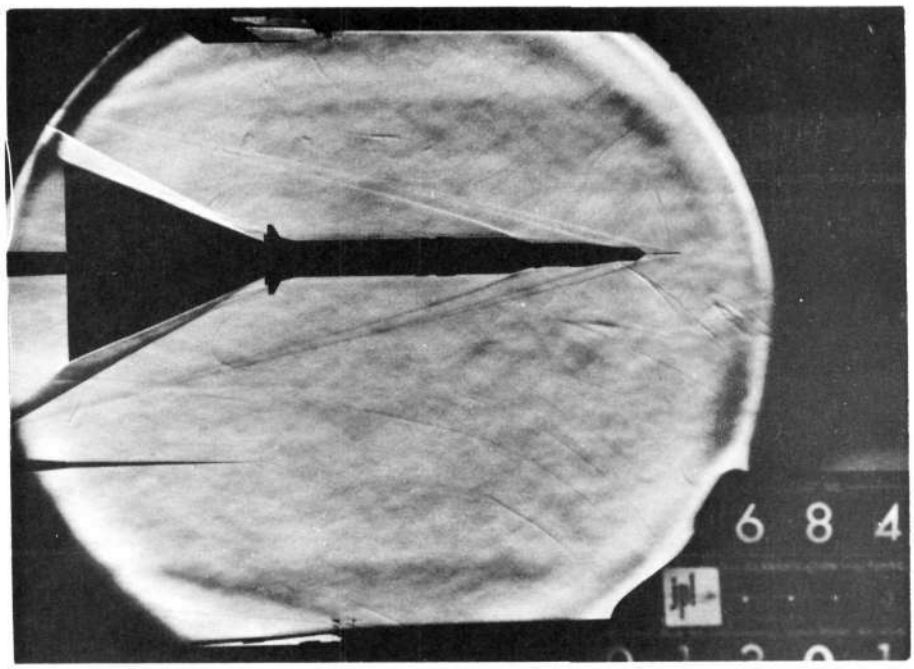

(c) M = 4.76

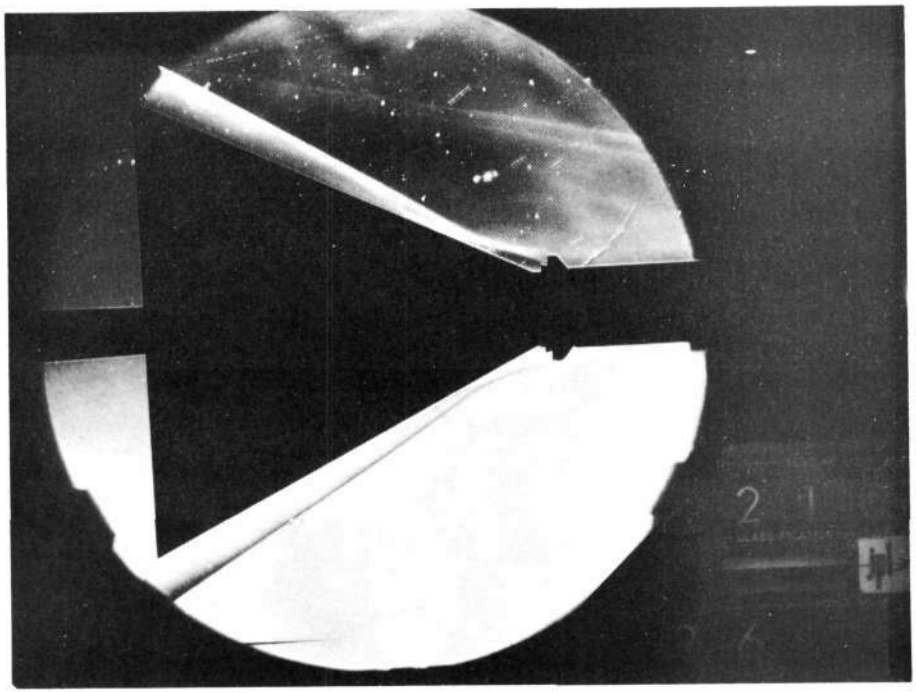

(d) M = 5.56

Figure 12.- Concluded.

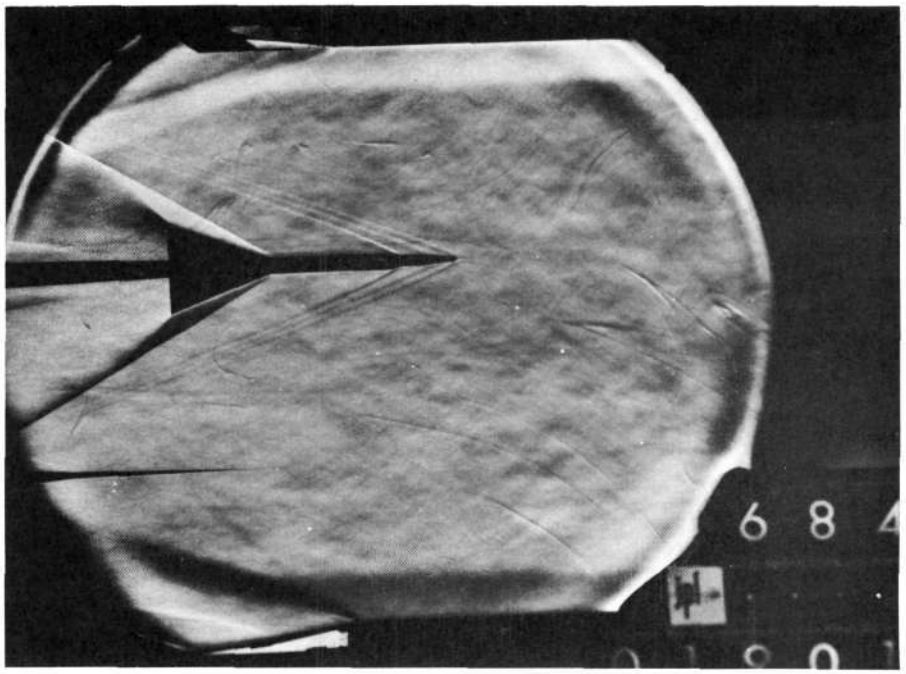

(a) M = 3.01

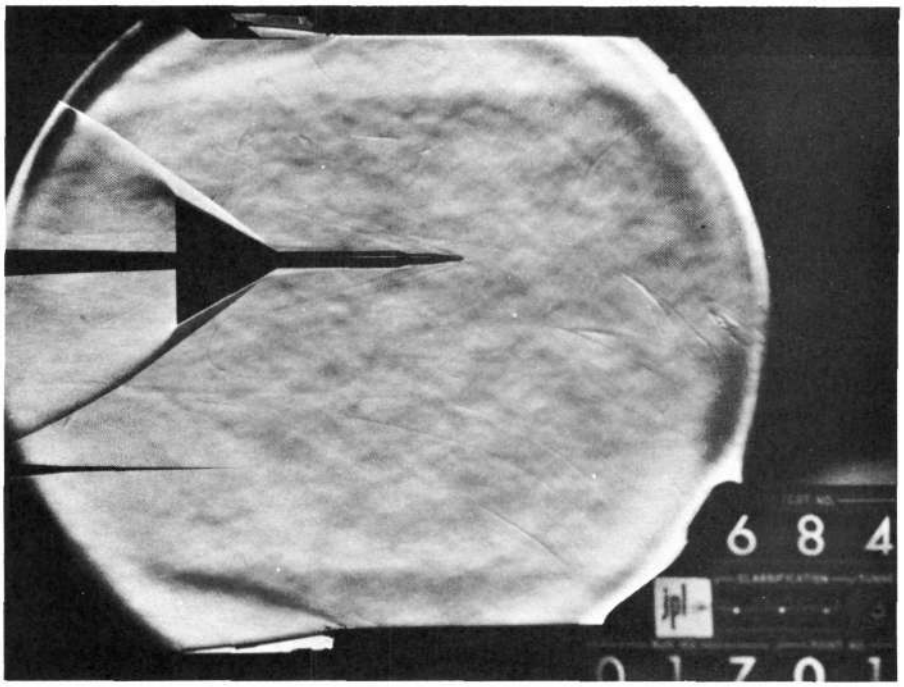

(b) M = 3.98

Figure 13.- Shadowgraphs of 0.00168-scale Saturn model, mixing boundary, plume; $\alpha = 0°$.

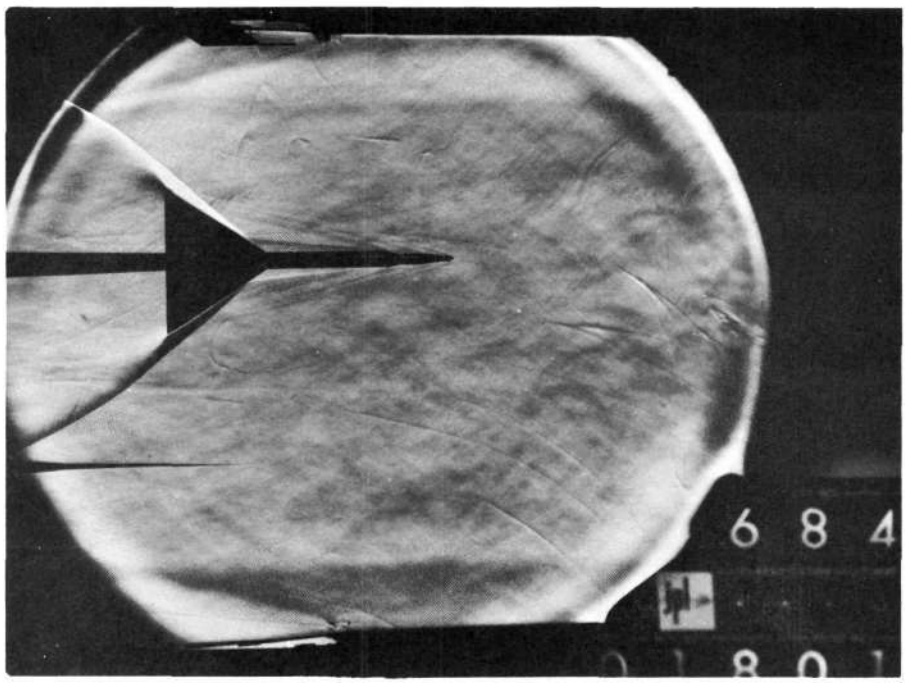

(c) M = 4.76

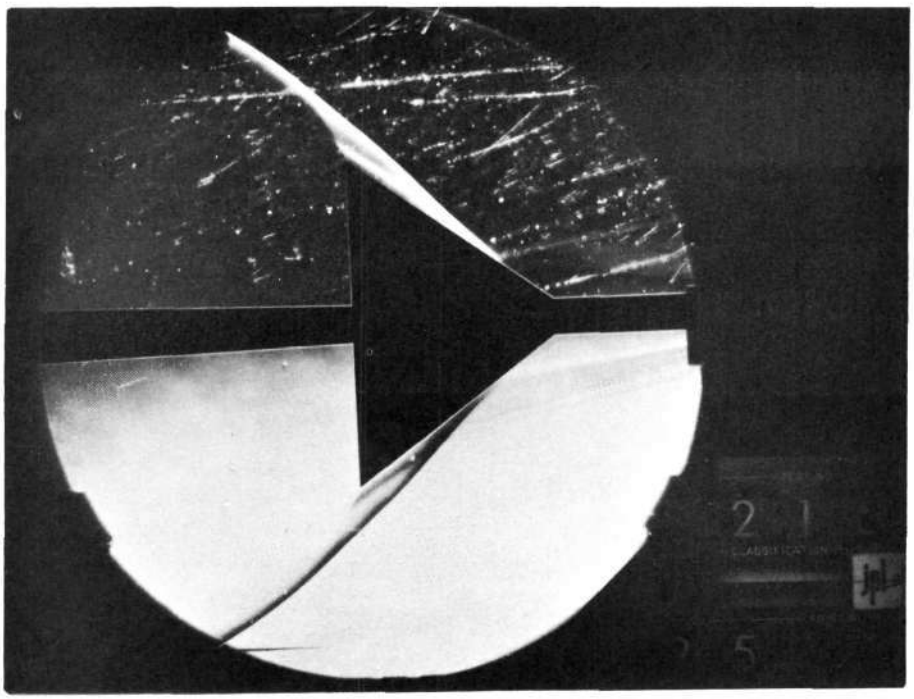

(d) M = 5.56

Figure 13.- Concluded.

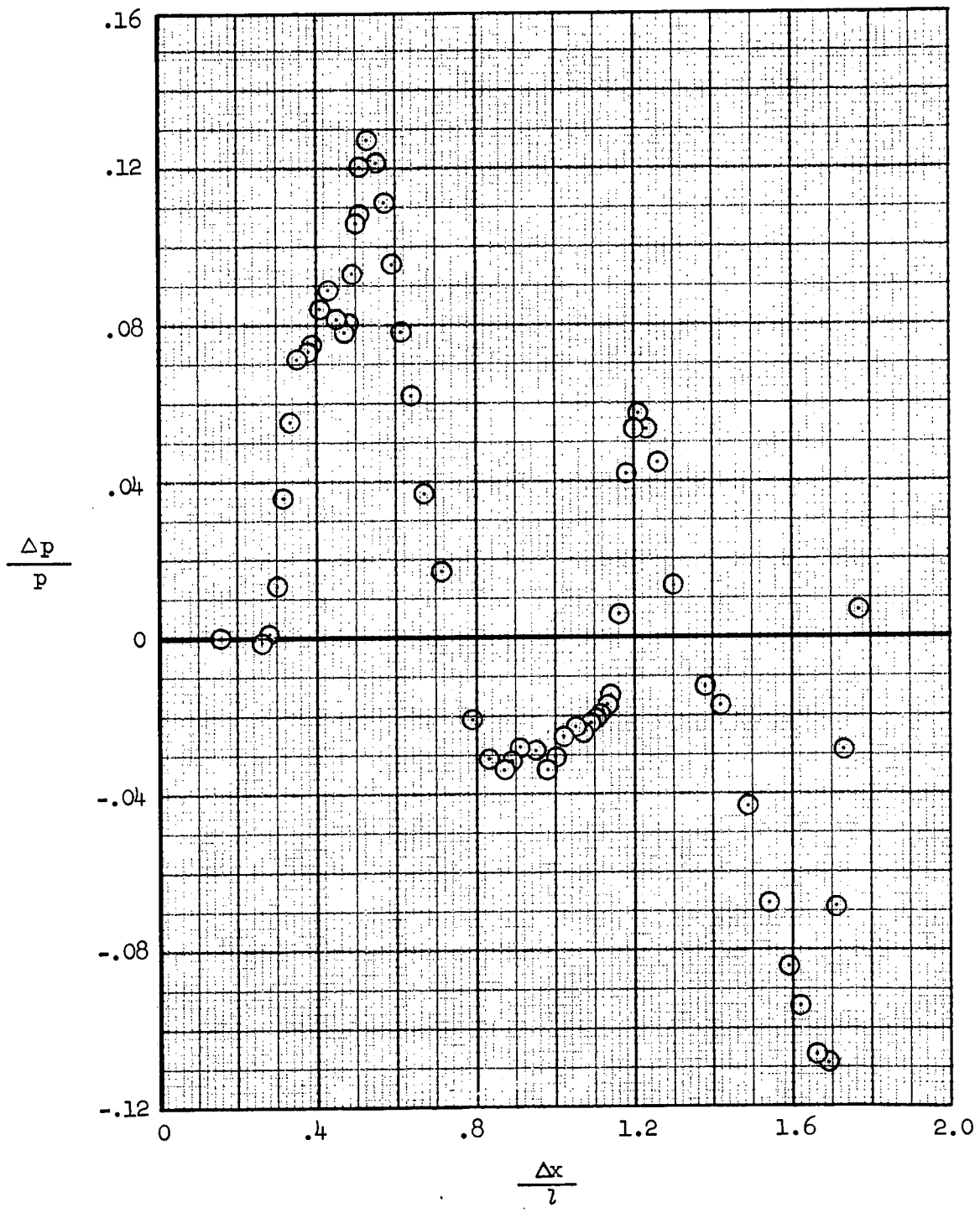

(a) M = 3.01, h/l = 0.57

Figure 14.- Wind tunnel pressure signatures for 0.00337-scale Saturn model; no plume, $\alpha = 0°$.

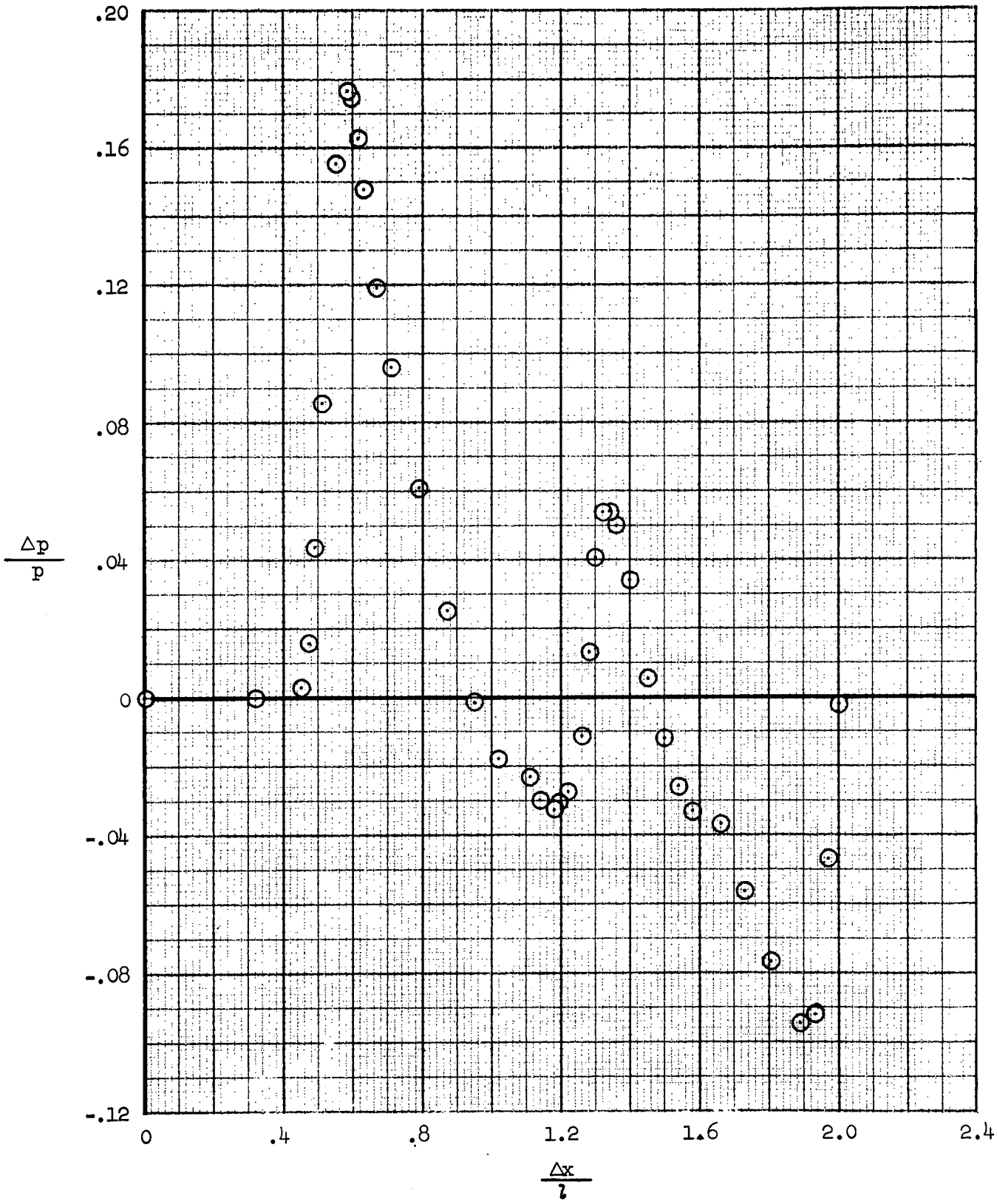

(b) M = 3.98, h/l = 0.57

Figure 14.- Continued.

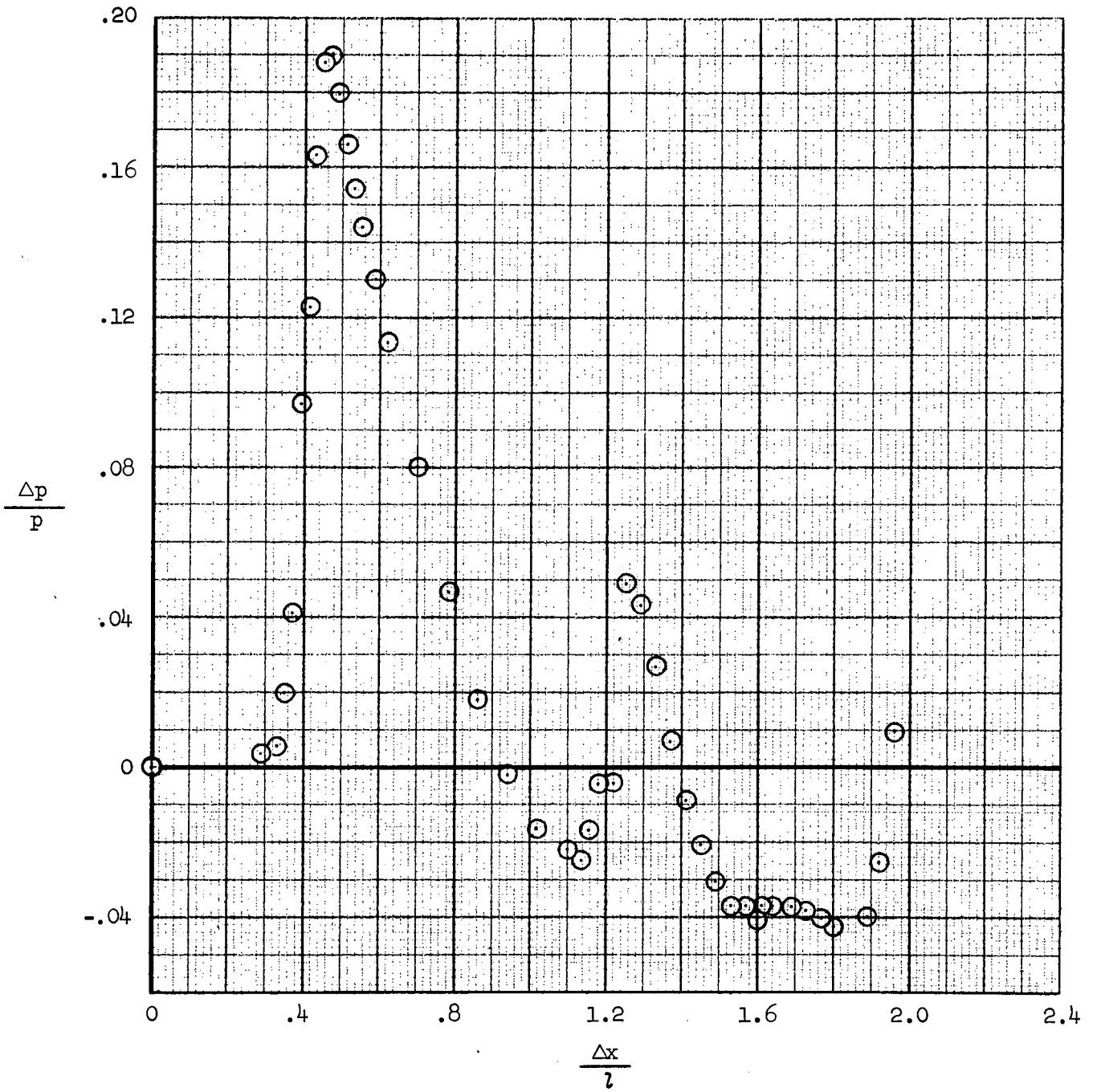

(c) M = 4.76, h/l = 0.57

Figure 14.- Continued.

D

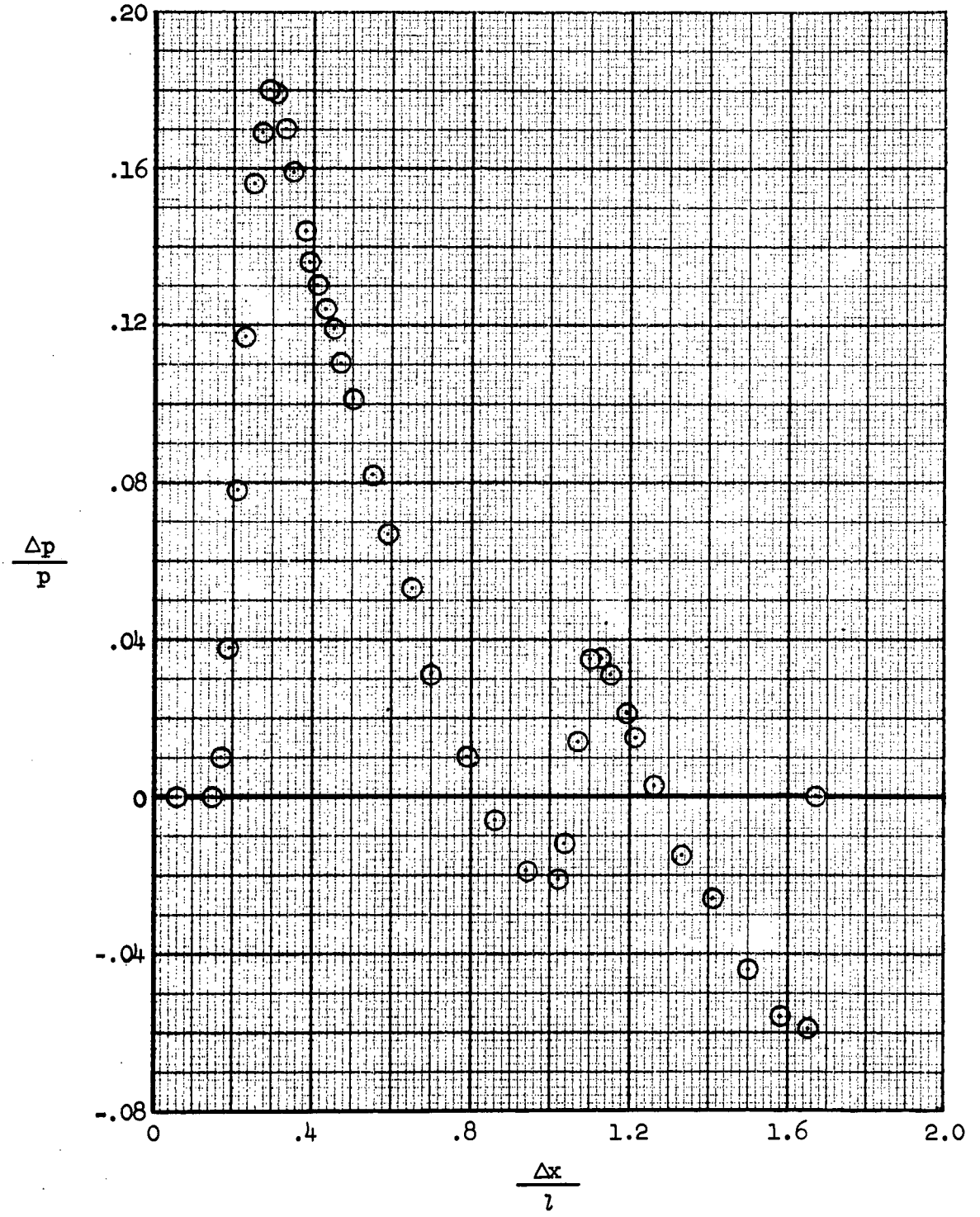

(d) M = 5.56, h/l = 0.63

Figure 14.- Continued.

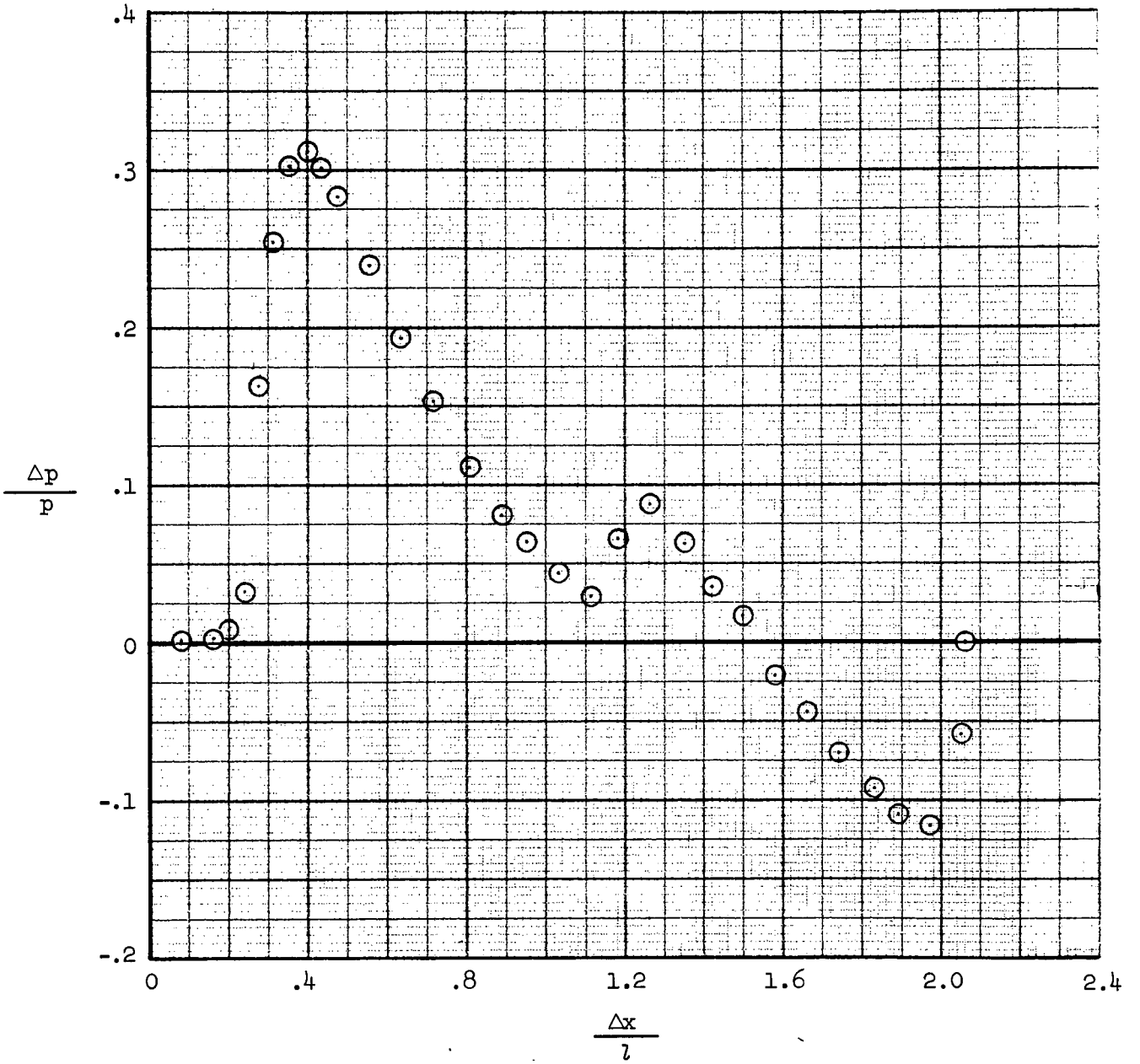

(e) M = 7.91, h/l = 0.47

Figure 14.- Concluded.

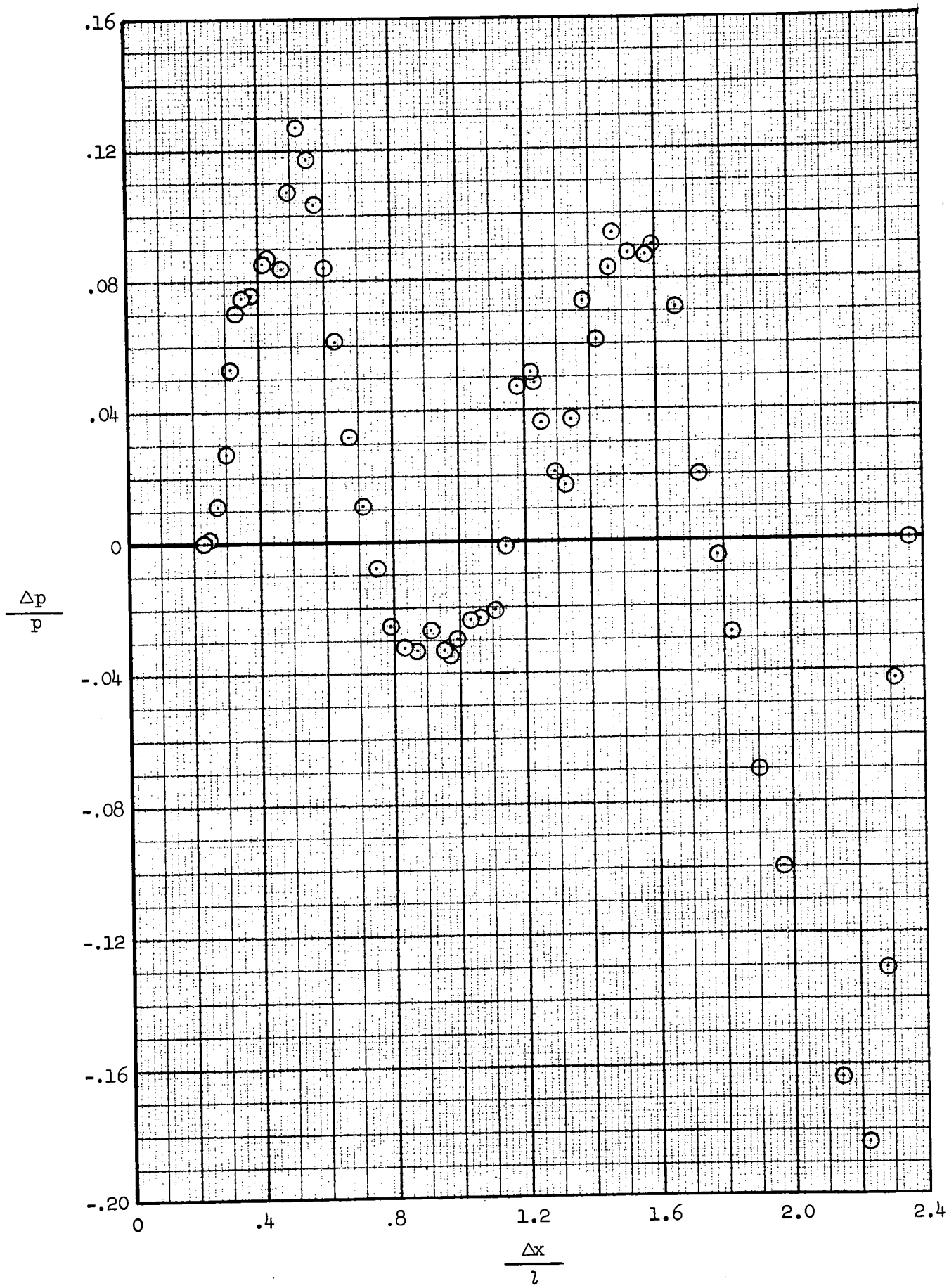

(a) M = 3.01, h/l = 0.57

Figure 15.- Wind tunnel pressure signatures for 0.00337-scale Saturn model; 2/3 inviscid boundary plume, $\alpha = 0°$.

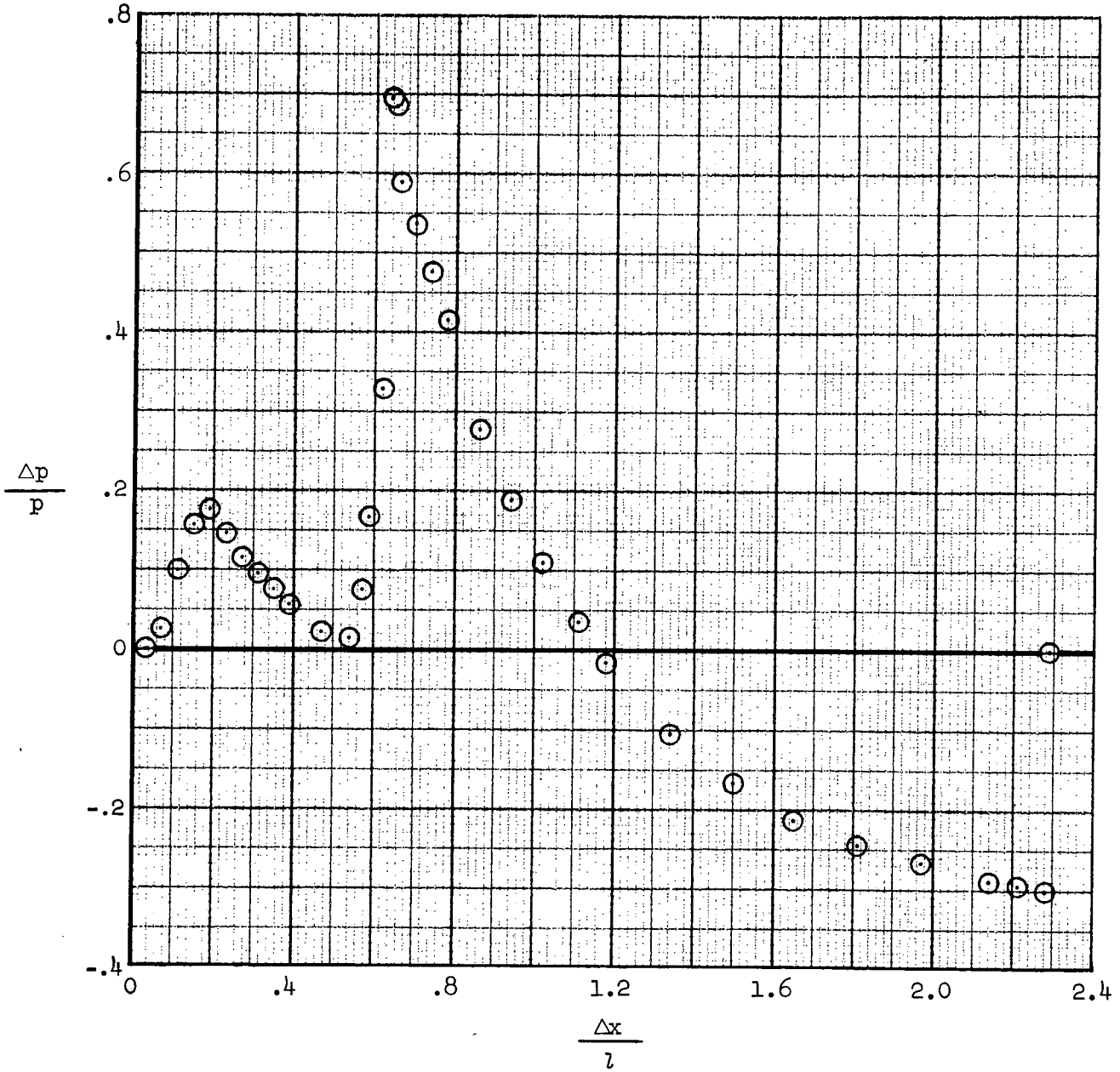

(b) M = 3.98, h/l = 0.57

Figure 15.- Continued.

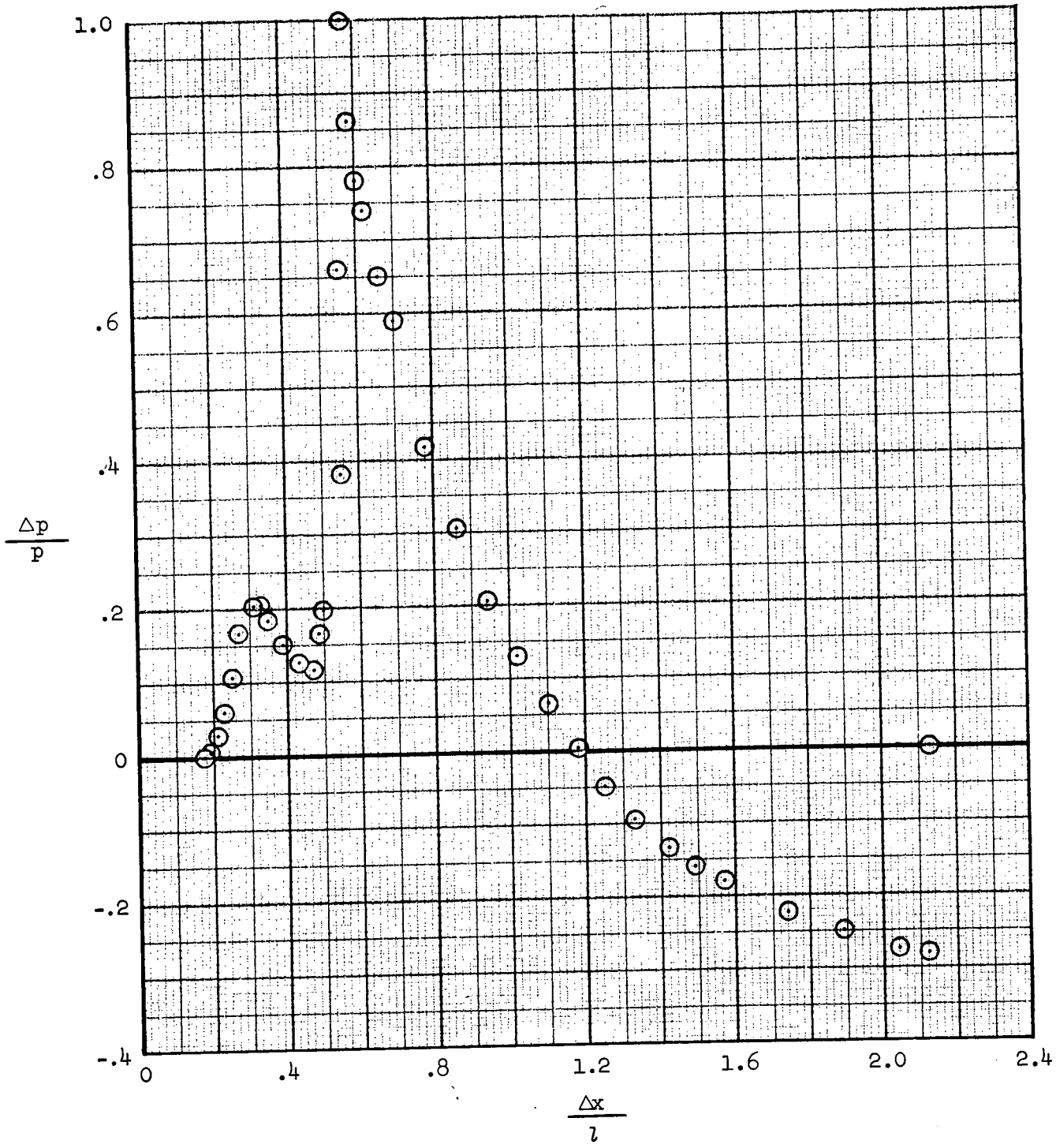

(c) M = 4.76, h/l = 0.57

Figure 15.- Continued.

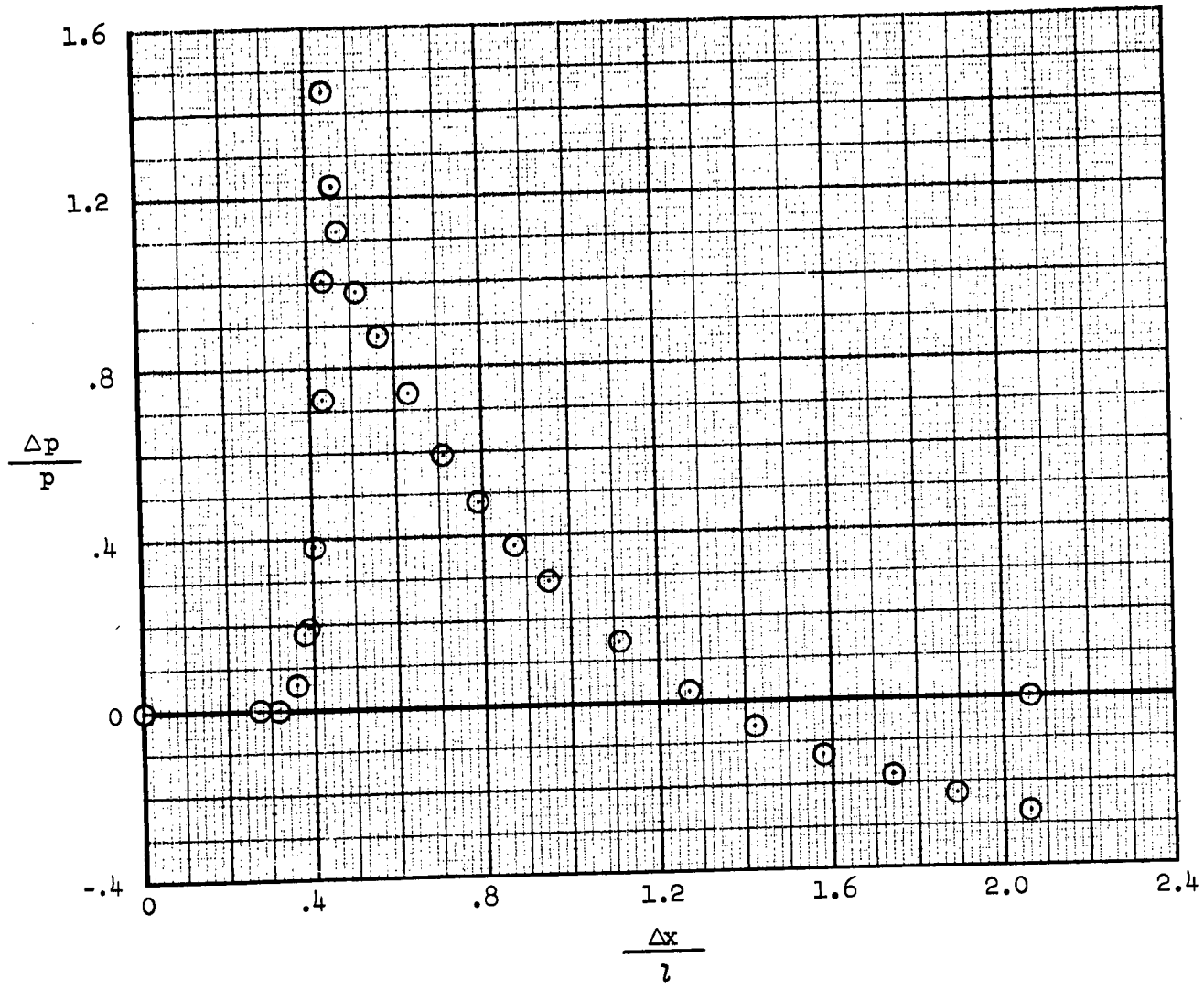

(d) M = 5.56, h/l = 0.63

Figure 15.- Concluded.

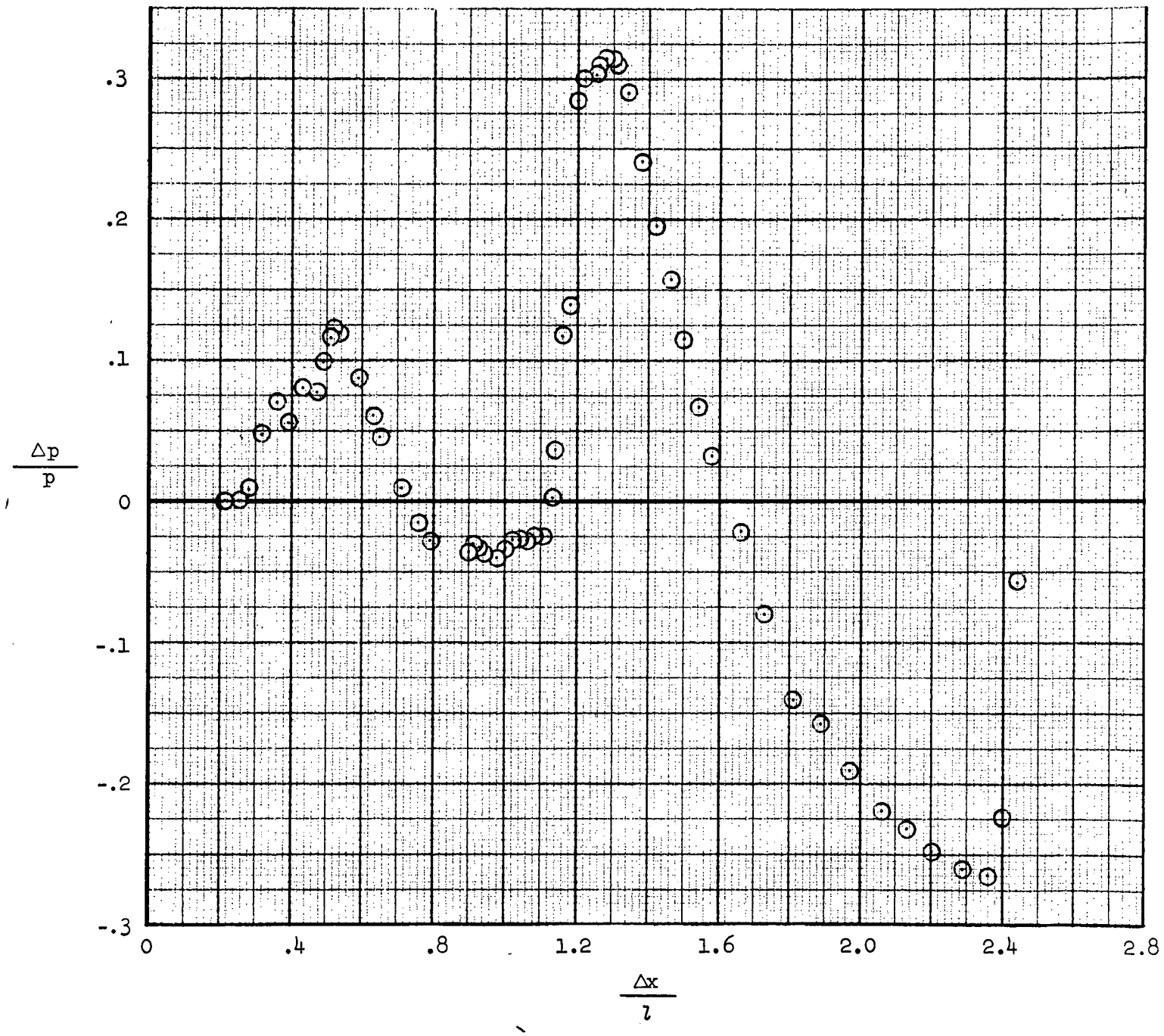

(a) M = 3.01, h/l = 0.57

Figure 16.- Wind tunnel pressure signatures for 0.00337-scale Saturn model; 2/3 inviscid boundary plume, $\alpha = 0°$.

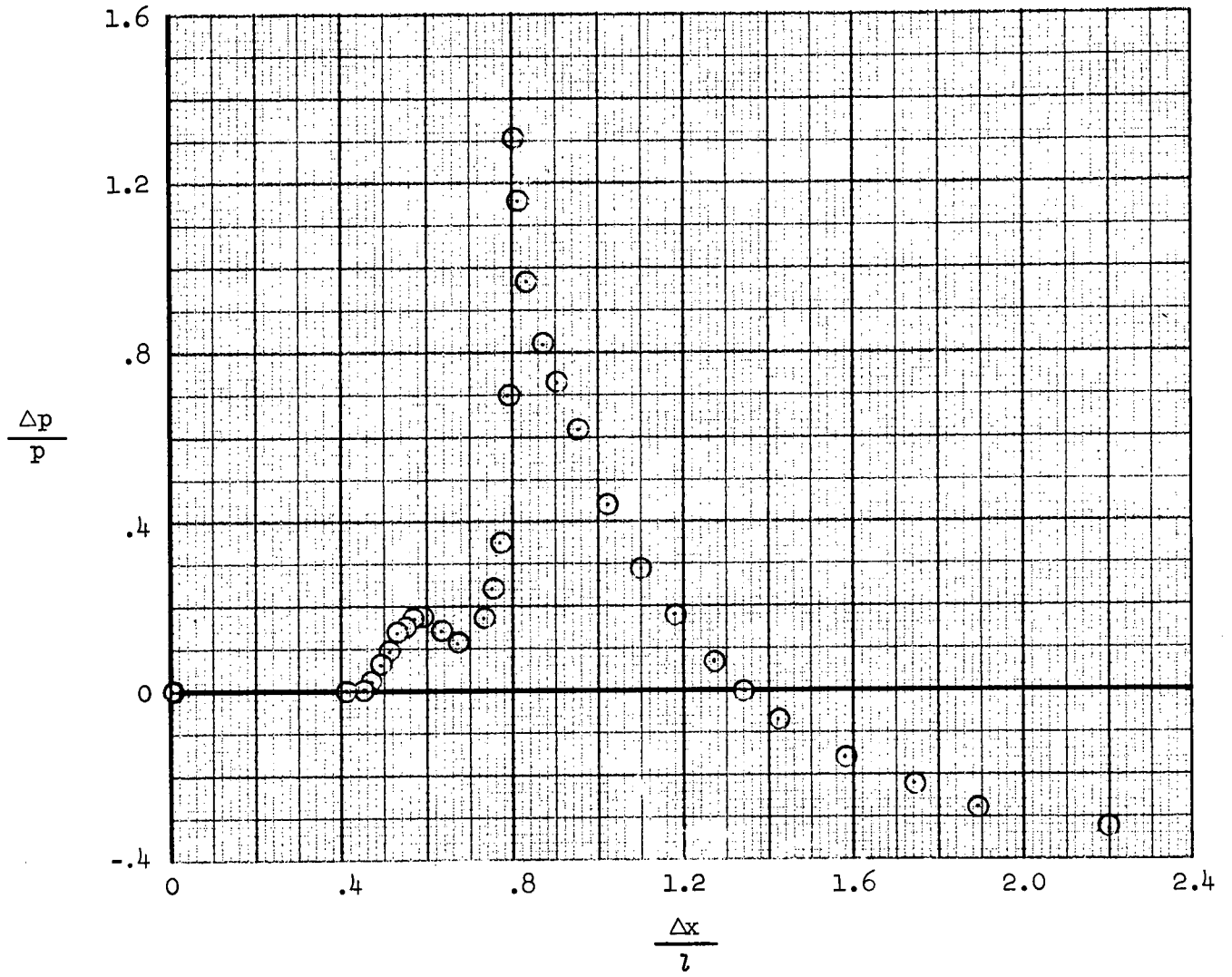

(b) M = 3.98, h/l = 0.57

Figure 16.- Continued.

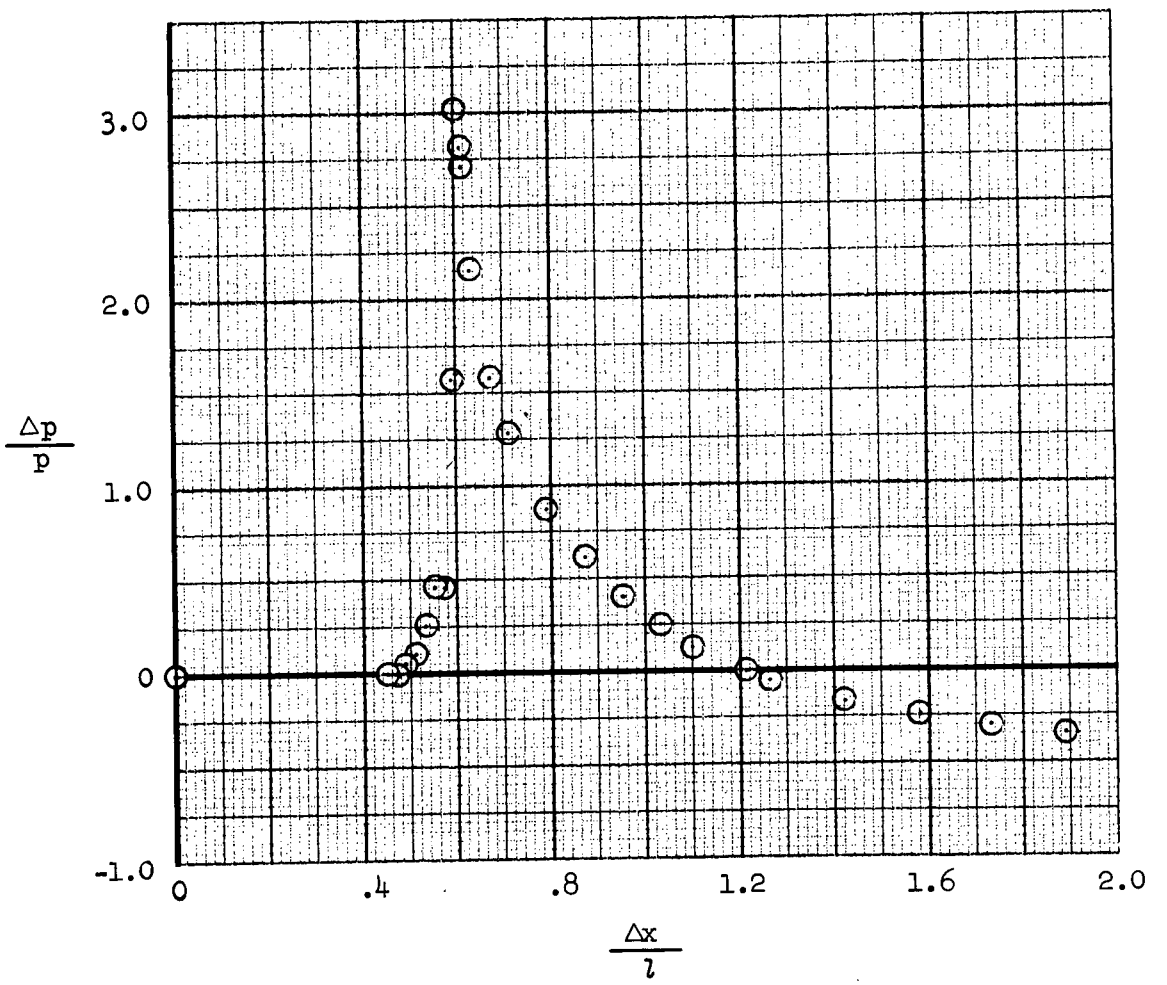

(c) M = 4.76, h/l = 0.57

Figure 16.- Continued.

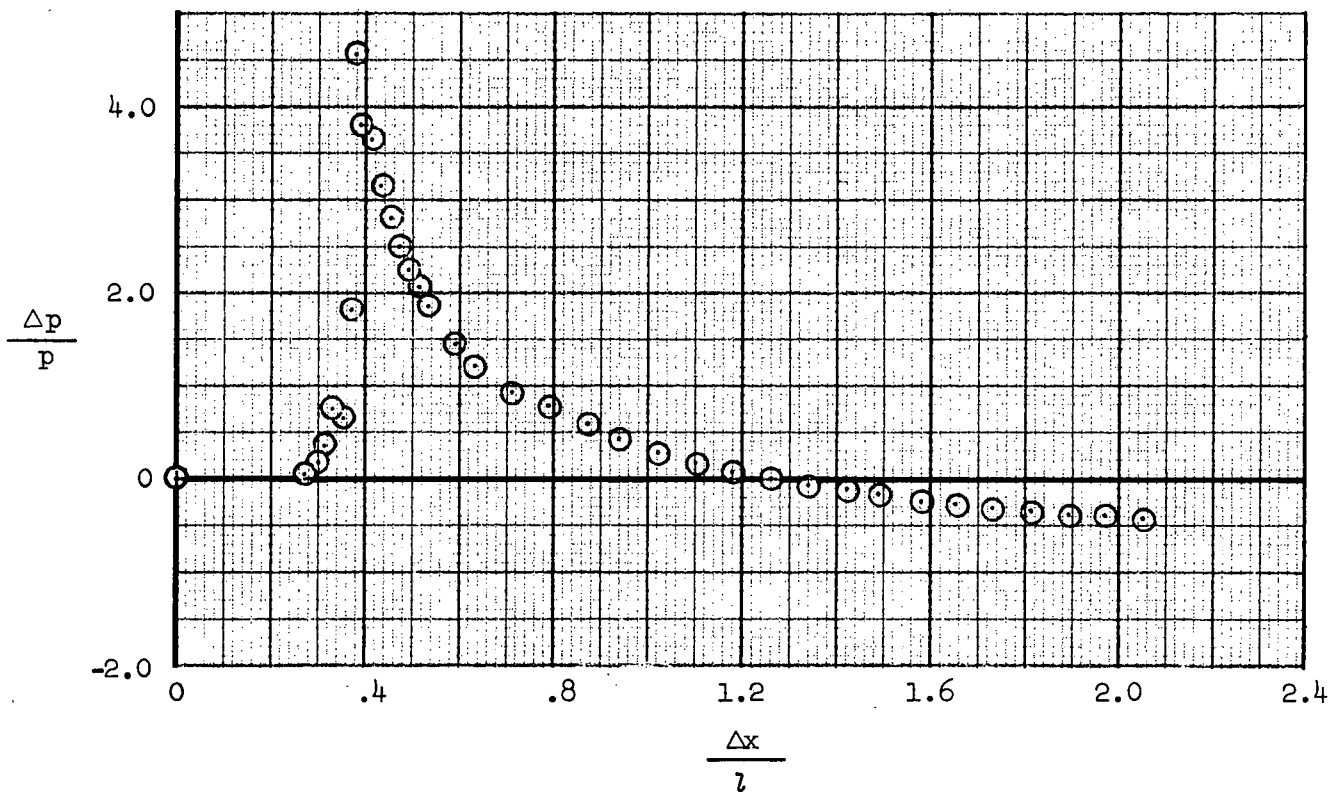

(d) M = 5.56, h/l = 0.63

Figure 16.- Concluded.

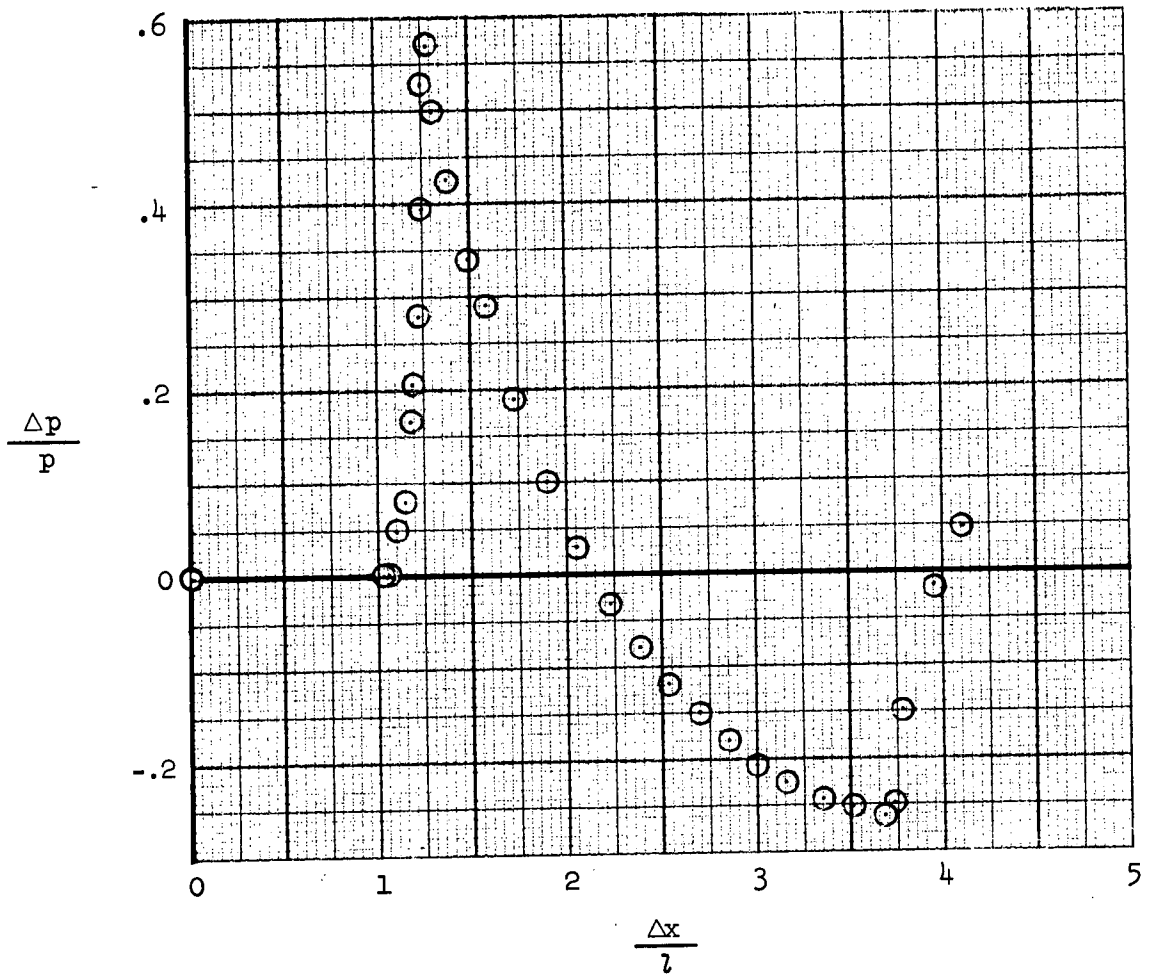

(a) M = 3.01, h/l = 0.57

Figure 17.- Wind tunnel pressure signatures for 0.00168-scale Saturn model; mixing boundary plume, $\alpha = 0°$.

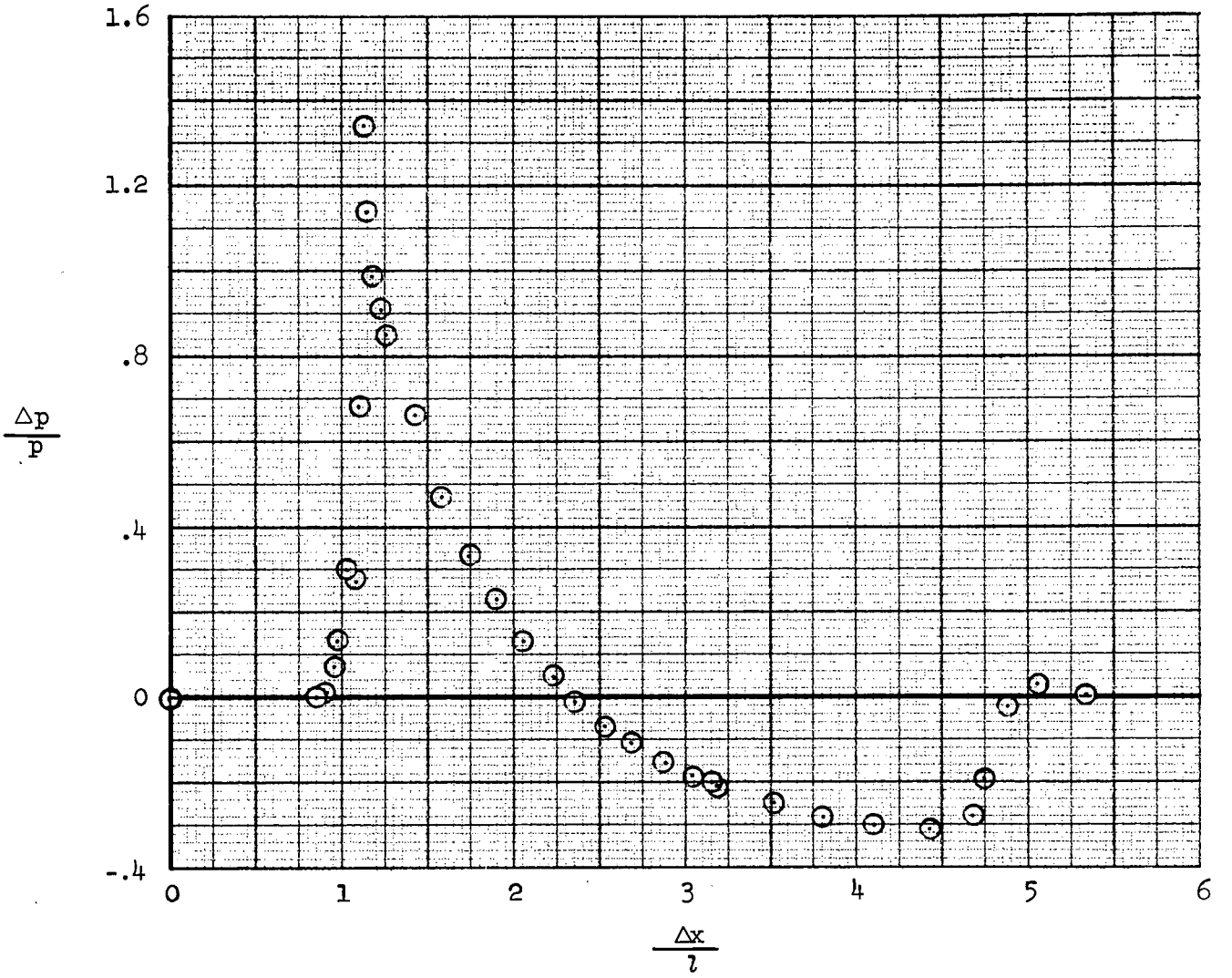

(b) M = 3.98, h/l = 0.57

Figure 17.- Continued.

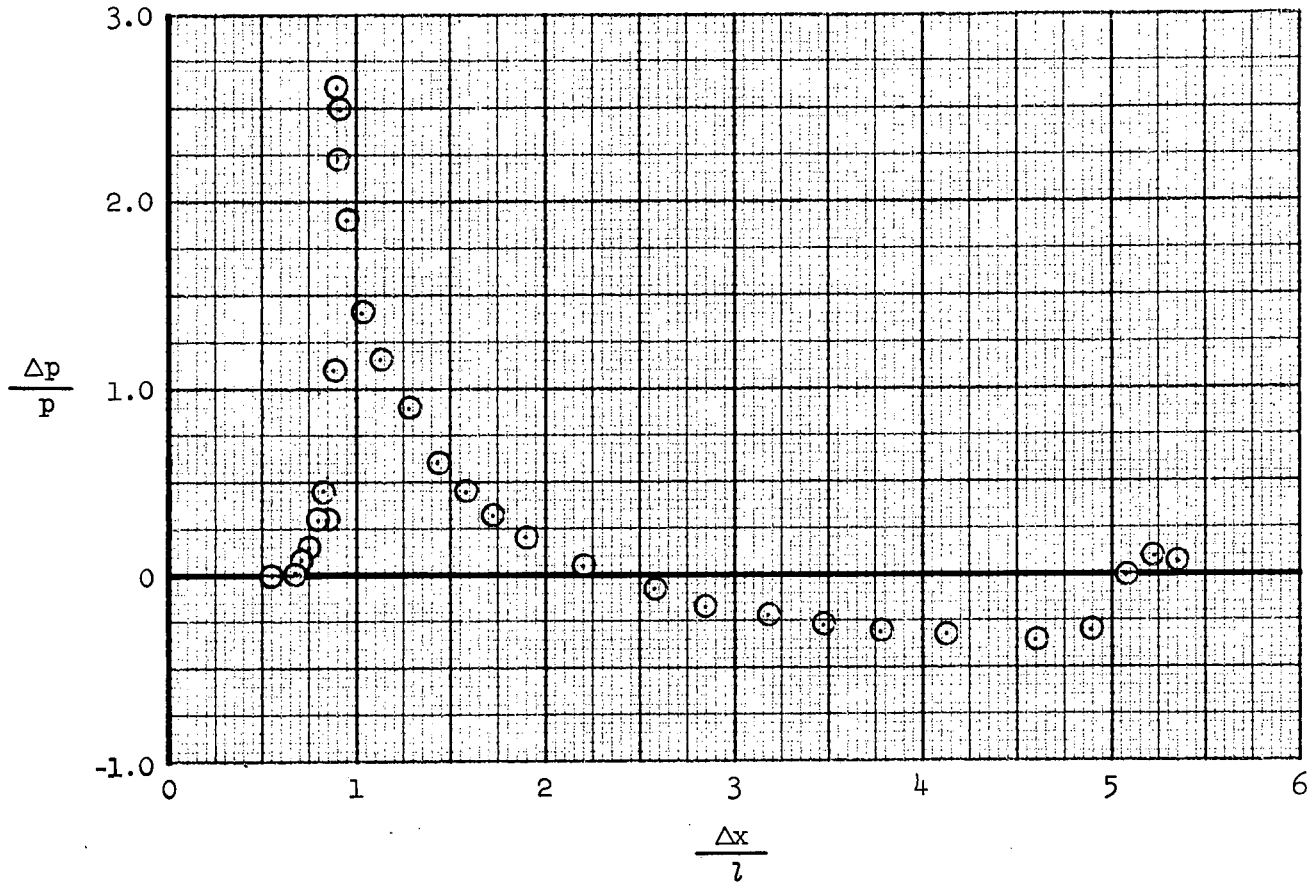

(c) M = 4.76, h/l = 0.57

Figure 17.- Continued.

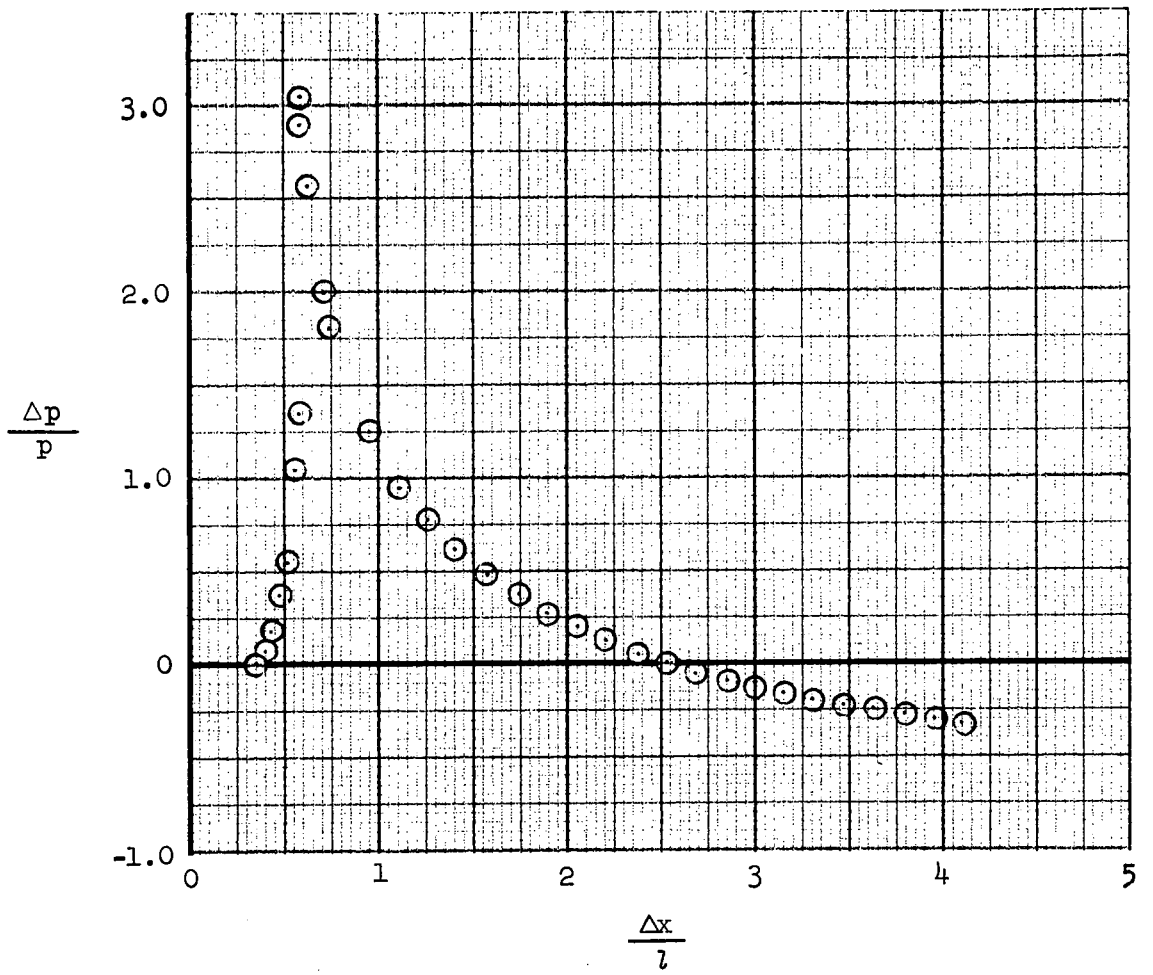

(d) M = 5.56, h/l = 0.63

Figure 17.- Concluded.

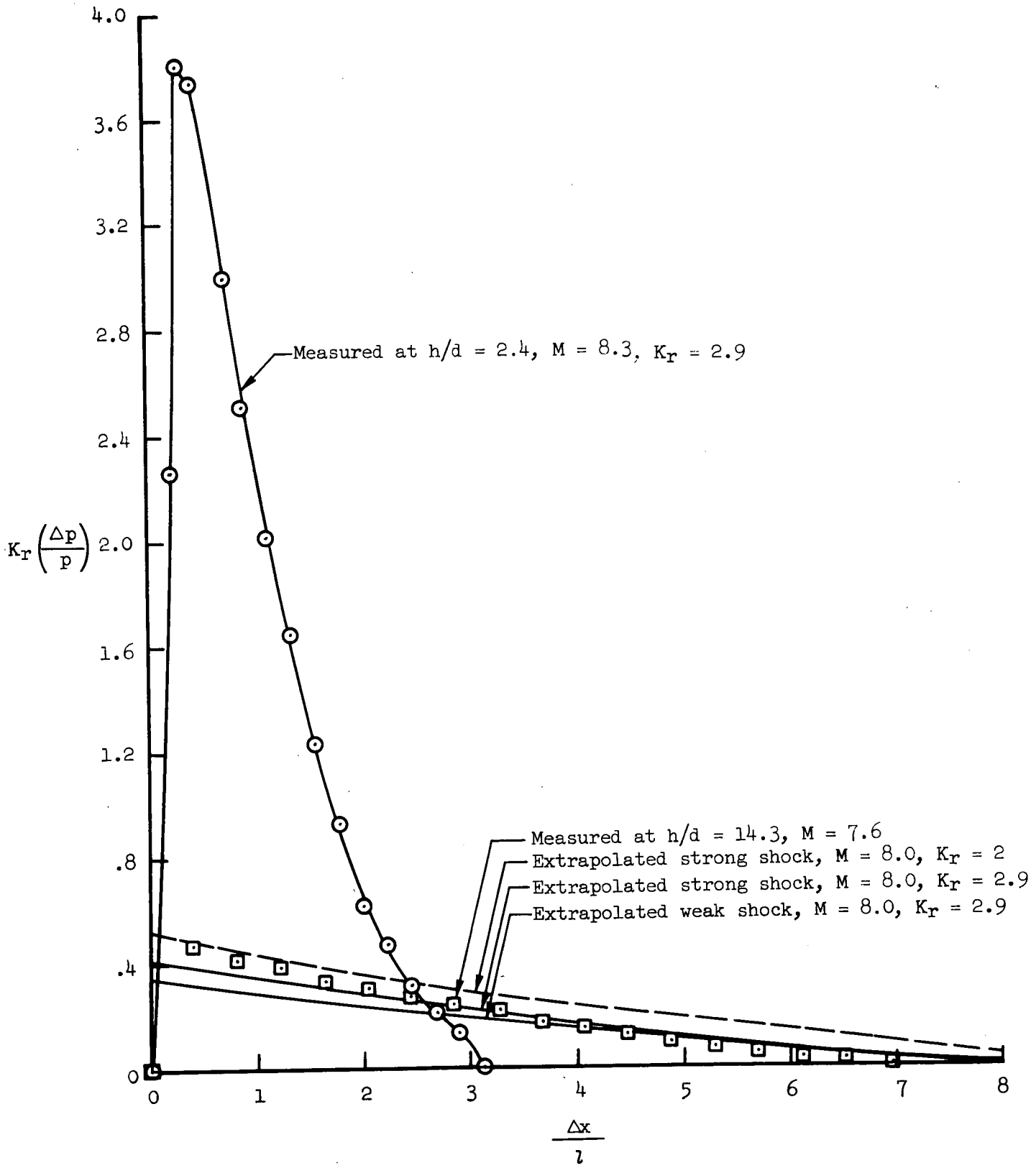

Figure 18.- Comparison of extrapolated and measured pressure signatures; ballistic range data for a sphere.

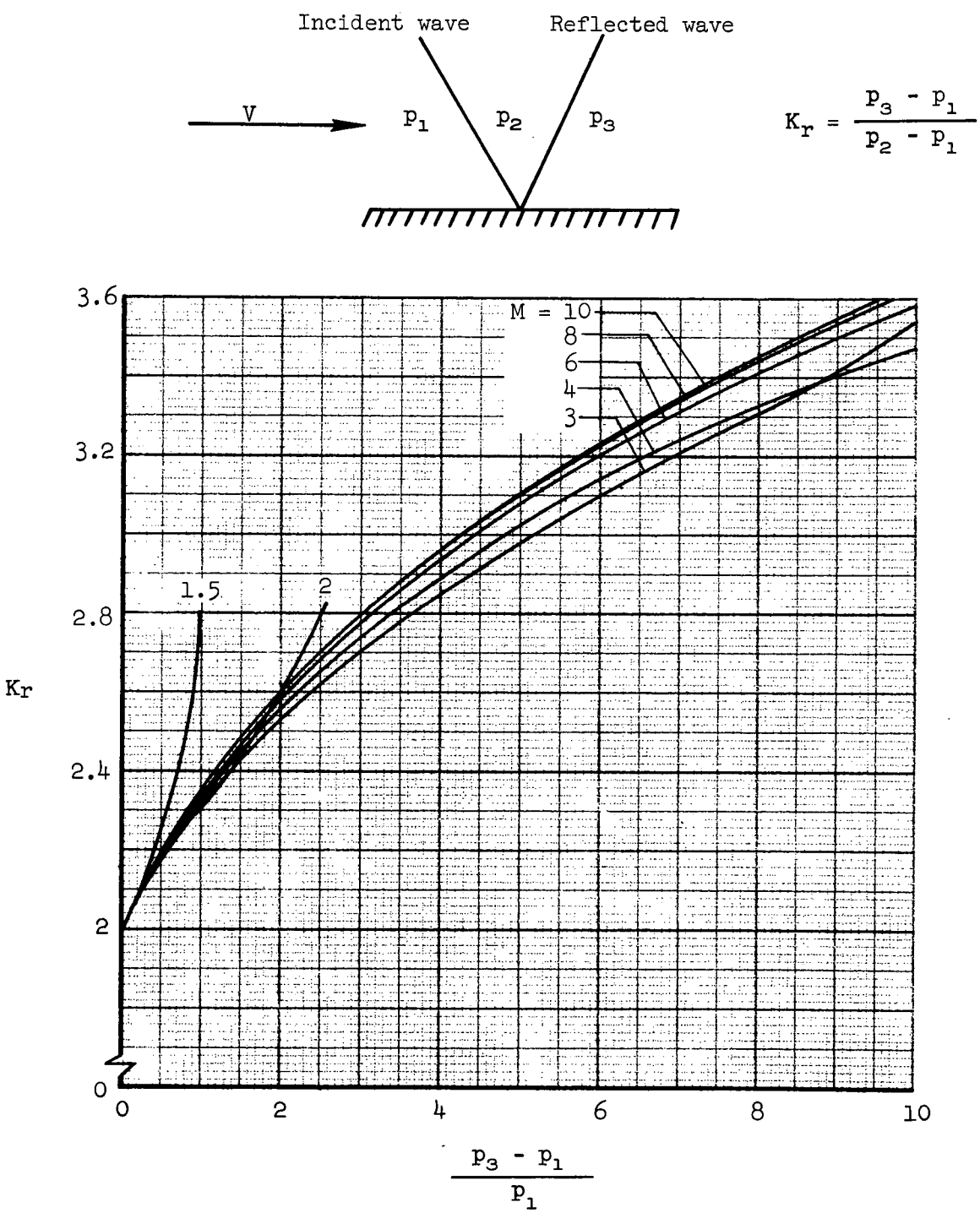

Figure 19.- Reflection factor vs total pressure jump.